THE EFFECTS OF THE INCORPORATED IMPURITIES AND THE OXIDE LAYER AT THE METAL-POLYMER CONTACT INTERFACE ON PARTIAL DISCHARGE AND BREAKDOWN PHENOMENA IN POLYETHYLENE

by

Dong Liu

A thesis
presented to the University of Manitoba
in partial fulfillment of the
requirements for the degree of
Master of Science
in
Electrical Engineering

Winnipeg, Manitoba, 1985

THE EFFECTS OF THE INCORPORATED IMPURITIES AND THE OXIDE LAYER AT THE METAL-POLYMER CONTACT INTERFACE ON PARTIAL DISCHARGE AND BREAKDOWN PHENOMENA IN POLYETHYLENE

BY

DONG LIU

A thesis submitted to the Faculty of Graduate Studies of
the University of Manitoba in partial fulfillment of the requirements
of the degree of

MASTER OF SCIENCE

ABSTRACT

The effects of an oxide layer at the metal-polymer interface on partial discharge and breakdown phenomena in polyethylene have been experimentally studied using a point-plane electrode configuration under various experimental conditions. The results show that the oxide layer on both the aluminum and iron point electrode surface increases the initiation voltage for partial discharges in polyethylene. The strong dependence of the discharge initiation voltage on the point electrode material, polarity of the voltage at the point electrode, the rise time of the applied voltage and the electrical stressing conditions is convincing experimental evidence that partial discharge is associated with carrier injection from the metallic contact and space charge formation by injected carriers trapped near the injecting contact. The interfacial oxide layer acts as a barrier and suppresses the direct communication between the carrier injecting contact and polymer, thus reducing the efficiency of carrier injection into the polymer. In polyethylene, hole injection is as feasible as electron injection from the point electrode.

On the basis of computer simulation of the polarity effects on the discharge patterns, it was found that the pattern is highly ramified when the point electrode is biased at the negative polarity indicating that the discharge is not only field-dependent but also governed by a stochastic process. The pattern is much less ramified when the point electrode is biased at the positive polarity, indicating that the discharge is governed mainly by a deterministic field-dependent process. These patterns reveal also that the partial discharge and breakdown processes are complex.

Breakdown phenomena are sensitive to impurities incorporated in the polymers. The breakdown strength for polyethylene films incorporated with nitrogen is higher, and that with silicon is lower, than that of pure polyethylene films; indicating that the breakdown strength depends on the energy level of the localized states created by the impurities in the energy gap.

We have also studied the effects of additives in polymers by measuring the conduction current through a polyethylene film between conductive fluid electrodes. The conduction current depends on the nature of ions contained in the fluid electrodes, indicating that the carriers are mainly ions produced by dissociation of the fluid molecules, and that these ions penetrate into the film as additives. They may

migrate following the electric field or else do not involve direct movement but have their protons transfered from molecule to molecule following the prototropic process. However, the additives in polymers change the inception voltage for partial discharge or breakdown.

All experimental results are discussed on the basis of Kao's model of electrical discharge and breakdown in low-mobility condensed insulators.

ACKNOWLEDGEMENTS

The author wishes to express grateful appreciation to his advisor, Professor K.C. Kao, for his excellent guidance, endurable motivation, consistent and generous support throughout the entire work; and also to Professors H.C. Card, D.M. Tu, F.Y. Liu, H.K. Xie, H.Y. Liu and X.L. Huang for their constant help and encouraging discussions.

Sincere thanks are given to his colleagues, S.R. Mejia, S.H. Kim, R.D. McLeod, W. Pries, P.K. Shufflebotham, Y.K. Hsieh, J.J. Schellenberg, J.F. White, H.C. Tse and other graduate students of the materials and Devices Research Laboratory and the staff of the Electrical Engineering Department of the University of Manitoba for their assistance and cooperation.

The author wishes to gratefully acknowledge the Ministry of Education of China and Xi'an Jiaotong University of China for the financial support of his M.Sc. studies in Canada.

CONTENTS

Chapter I

INTRODUCTION

Rigorous pioneering work in the field of polymers was started by the Nobel Laureate Staudinger in 1920, Freadenberg in 1921, Meyer and Mark in 1928 and many others. Since then, the research and development of the field of polymers have been rapidly growing, particularly after the discovery of polyethylene methacrylate in 1930 by Hill and Crawford, and polyethylene in 1932 by Gibson and Swallow. Now synthetic polymers are used extensively as electrical insulators because of their good electrical and mechanical properties. They have a wide variety of applications ranging from power apparatus and cables to microelectronics. Electrical engineers are concerned with the utilization and behaviour of a wide variety of insulating materials over an ever broadening range of electric stresses, frequencies, temperatures and other operating conditions. In the field of electronics, new applications of polymers continue to arise in the area of computer data storage, such as the holeburning memory properties of polyethylene derivatives recently developed by IBM researchers.

A key to future progress in applications of polymers is the fundamental understanding of their electrical and optical properties. These properties for polymers have therefore been a target of intensive research. The most important electrical properties of polymers for insulating applications are the breakdown strength and the threshold voltage for the onset of internal partial discharges.

There is ample evidence that a dielectric failure may have been preceded by a long progressive development of one or more minute branched hollow channels created by partial discharges, which are generally refered to as an electrical tree[1,2]. It is now generally accepted that tree formation is the main cause leading to the final failure of polymeric insulating cables and power apparatus. Several mechanisms have been put forward for the initiation of an electrical tree, mainly (1) mechanical fatigue, (2) partial discharges, and (3) charge injection and extraction. It is generally believed that mechanism (3) is the most important process[3]. If mechanism (3) is true, then the treeing properties will depend on the electrode material used, and therefore carrier injection is one of the most important factors in determining the treeing phenomena. In practice, the surfaces of most metallic electrodes contacting the polymeric material may have been oxidized, forming a thin oxide layer blocking intimate contact between the metal and the polymer. This may affect the efficiency of carrier

injection. However, little has been reported about oxide layer effects on the treeing properties. In order to better understand the effects of the metallic electrode material and oxide layer at the interface on the tree initiation process, we have measured the tree initiation voltage (Vt) and the tree penetration length with and without a thin oxide layer at the metallic-polymer interface under different electrical conditions. In Chapter III , we shall present some new results about these effects.

Recently, there has been a wealth of interest and activity in describing natural phenomena using fractal geometry [4]. Some recent computer simulations involving fractal geometry include the observation of fractal geometry in pattern of dielectric breakdown [5]. Niemeyer, Pietronero and Wiesmann [5] have recently reported a nontrivial stochastic model based upon the field dependence of the branching probability in the discharge pattern. We have found that the discharge pattern is polarity dependent using a point-plane electrode configuration. Based on their model, we can also describe these polarity dependent patterns. This will be presented in Chapter IV.

Over the past ten years much attention has been paid to impurity effects on insulating polymers. Since most industrial polymers contain various organic and inorganic impurities such as catalysts, antioxidants, voltage stabilizers

etc., it is likely that the electrical properties may have been modified by such impurities. The impurities can be divided into two general kinds with respect to their states in polymers: (i) impurities incorporated into the polymer, and (ii) impurities added to the polymer as additives to form a non-reactive physical mixture.

Theoretically, a suitable impurity incorporated in a polymer may change it from an insulating polymer to a conducting or semiconducting polymer [6]. Of course, impurities may also affect the dielectric properties of the polymers. In order to find how incorporated impurities can affect the breakdown properties, we have measured the breakdown voltage of the polyethylene thin films incorporated with nitrogen and silicon. These results are given in Chapter V.

Some investigators [7,8,9] have also reported that additives can raise the inception voltage for the onset of electrical trees. Many dielectric liquids have been investigated for the use as such additives. It is generally believed that the action of additives is a stress grading process activitied either by field enhanced dissociation [8,9] or by field enhanced ionization [10]. For these complex phenomena more work is required for a better understanding of the effects of the additives. We have carried out an investigation into this problem from a different

angle by studying electric conduction in polyethylene between conductive fluid electrodes in the hope that this experiment can simulate additives in polyethylene, and provide further insight into the behaviour of additives in polymers. In Chapter VI we shall present our new results and new approach to the mechanism responsible for the electrical tree inhibition by the additives in polymers.

As a great deal of work in this field is available in the literature, a brief review of present knowledge about oxide layer effects on the electrical treeing properties of polyethylene, and the effects of additives and doped impurities on the properties of polymers is desirable. Such a review is therefore given in Chapter II. Conclusions arising from the present investigations are given in Chapter VII.

Chapter II

REVIEW OF PREVIOUS WORK ON ELECTRICAL DISCHARGE AND BREAKDOWN PHENOMENA IN POLYMERS

In the past few years several extensive review articles and books in the field of polymers have been published [11,12,13]. In this Chapter, only a brief review on the work relevant to the present investigations is given; this includes electrical treeing, interfacial phenomena and effects of impurities with particular emphasis on the work which has not been included in the aforementioned review articles.

2.1 BREAKDOWN THEORIES

The first breakdown theory of solid dielectric was put forward by Wargner [14] in 1922. In this theory, dielectric breakdown occurs when the Joule heating produced by the conduction current is equal to or higher than the energy dissipated in the material. This thermal breakdown theory can explain the dielectric breakdown phenomena in the high temperature region, but it becomes invalid in the low temperature regions. Since then, several investigators have suggested that the dielectric breakdown of solids can also

be due to electrical processes such as current multiplication by collision ionization of high energy electrons, as in gasses. These suggestions are based on experimental results such as time lag and the direction of the breakdown path etc.[15,16]. Thus the interactions between hot electrons accelerated by the applied electric field and phonons attracted much interest as a subject of theoretical physics in 1940 to 1950 [17,18,19,20].

After 1950, a number of different breakdown theories were put forward according to differences in the approximation and energy exchange processes. Among them, the important ones are: (a) the transfer of the energy of hot electrons gained from the electric field to the lattice (electron-phonon interaction) so as to increase the lattice temperature to a critical value, at which a permanent change in lattice may occur, (b) the internal field emission induced by high fields (Zener breakdown), and (c) the impact ionization at high fields. Breakdown mechanisms were first studied for the alkali halide single crystals and crystalline silicon P-N junction whose structures are relatively simple. These breakdown theories of dielectric solids are listed in Table 2.1.

However these theories are not good for low-mobility condensed insulators, such as polymers, since in low mobility materials: (i) the carrier mobility μ is less than

Table 2.1 Dielectric Breakdown Theories of Solids

I. Electronic breakdown process

- Intrinsic breakdown ($\partial F_B/\partial d = 0$; d: sample thickness)
  - Theories based on the single electron approximation ($\partial F_B/\partial T \gtrsim 0$)
    - High energy criterion
    - Low energy criterion
  - Collective critical field theories
    - Single crystal ($\partial F_B/\partial T > 0$)
    - Amorphous materials ($\partial F_B/\partial T < 0$)
- Electron avalanche breakdown ($\partial F_B/\partial d < 0$; $\partial F_B/\partial T \gtrsim 0$)
  - Single avalanche model
  - Collective avalanche model
- Field emission breakdown ($\partial F_B/\partial d = 0$; $\partial F_B/\partial T = 0$)
- Free volume breakdown ($\partial F_B/\partial T < 0$)

II. Thermal breakdown process

- Steady state thermal breakdown ($\partial F_B/\partial T < 0$)
- Impulse thermal breakdown

III. Mechanical breakdown process

- Electromechanical breakdown ($\partial F_B/\partial T < 0$)

$10^{-1}cm^2/V \cdot s$, (ii) the energy band gap Eg is larger than 4 eV and (iii) the localized gap state concentration is much larger than the thermal equilibrium carrier concentration. Because of these different features, it is almost impossible for carriers to gain enough energy from the field to become sufficiently hot to cause structural changes in the material, which means that avalanche breakdown is impossible at the beginning. Also, the Zener process is impossible since the tunneling probability for electrons is negligibly small in a low mobility material. Base on these facts, Kao [21] has proposed a new theory of electrical breakdown in low mobility condensed insulators.

Kao's theory is different from conventional theories. According to his theory, the electrons injected from the electrode will be trapped or recombined after one or a few scatterings because of a small mean free path and large localized gap state concentration. In a transition from an upper to a lower energy state an energy equal to the energy difference between the two states will be evolved either radiatively or non-radiatively. In non-crystalline insulator such a transition is mainly non-radiative. Since low mobility materials always have a high energy gap, this released energy will be the order of 4 eV - 5 eV. This energy will make another electron in the conduction band become a hot electron which then has sufficient energy to bombard a molecule and break its bonds. The bond energies

are of the order of 3.5 eV to 3.8 eV [21]. This process will create a low density region in the polymers. After the formation of a low density region, impact ionization may occur in this region when the field, the mean free path, and the ionization energy of the radicals in the region are at appropriate values.

The main differences between this model and the conventional ones are: (a) The energy of the hot electron is generated by an Auger type process as shown in Fig. 2.1 and is not gained from the field. (b) The impact ionization takes place in the low-density region and not in the material itself. Kao's theory can explain almost all breakdown phenomena observed in low mobility condensed insulators. The breakdown path is always filamentary irrespective of the material phase indicating that the carrier injection efficiency varies from site to site on the injecting electrode surface.

The breakdown strength of polymers is strongly dependent on temperature. It is possible to divide the breakdown strength temperature characteristics into three regions [22]. Region I is for low temperatures to room temperature. In this region the polymer is glass-like, and the corresponding breakdown process is electronic. Region II is for room temperature to the temperature before the melting point. In this region the polymer is rubber-like, and the

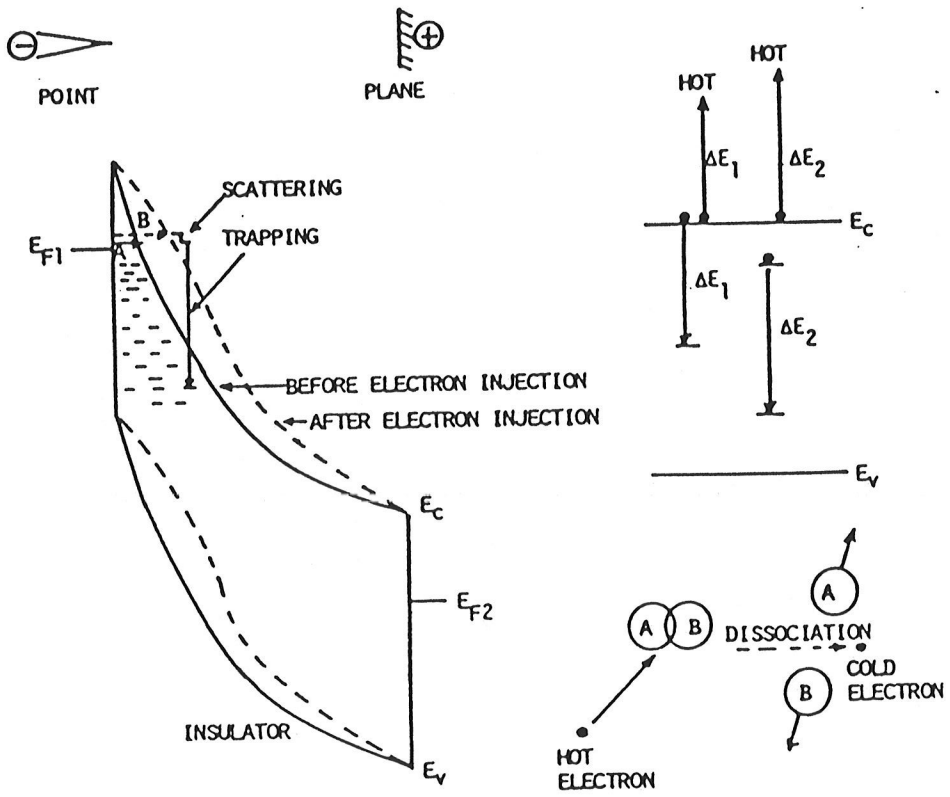

Fig. 2.1A: Illustrating electron injection, electron trapping, buildup of homospace charge modifying internal field distribution (A before and B after electron injection), hot electron generation process, and dissociation of a molecule into radicals by hot electron bombardment for the point electrode at negative polarity. The scale is exaggerated for clarity. (After Kao [21]).

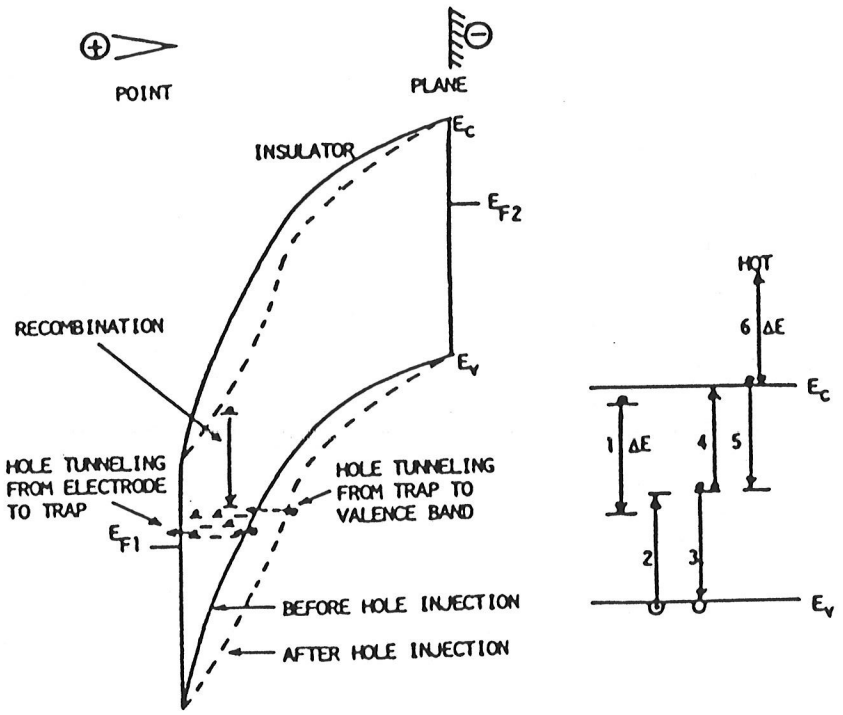

Fig. 2.1B: Illustrating hole injection, trapped electron-trapped hole recombination, buildup of homo-space charge modifying internal field distribution and hot electron generation process for the point at positive polarity. The scale is exaggerated for clarity. (After Kao [21]).

corresponding breakdown processes involve both electronic and thermal processes, including the effect of free volumes. Region III is for temperatures above the melting point. In this region the polymer is said to be in the plastic-flow state, and the corresponding breakdown process is thermal and electromechanical.

2.2 ELECTRICAL TREEING PROPERTIES AND MECHANISMS OF TREE INITIATION

At the present time the most widely used insulating materials are organic polymers. Because of the morphology of polymers, all of the charged components are not equally well anchored and failure always take place at the weakest point, when the specimen is subjected to high field. Typical failures are small channels pierced from one electrode to another electrode. These initiation discharge channels are referred to as an "electrical tree". To study electrical treeing properties, a point-plane electrode configuration is generally used to simulate the localized high field points in the insulating material.

About twenty years ago, a number of investigators such as Kitchin [23], Olyplant [24], McMahon [25], Vahlstrom[26] and Lawson [27] etc. have reported that polyethylene insulated power cables which failed in service contained electrical trees. Since then, the electrical treeing properties and the mechanisms for their initiation have been

extensively studied. Some of the mechanisms are now summarized as follows:

(a) Trees are initiated by mechanical fatigue. The high Maxwell compression force on the dielectric caused by the high voltage stress at the point electrode produces a fatigue cracking of the polymers [28].

(b) Trees are initiated by partial discharges. This is based on the belief, supported by experimental evidence, that small cavities [30] can exist at tips of foreign particles, asperities of point due to differential thermal expansion of the polymer and metal or adsorbed or occluded gas on the surface. But careful tests with point electrodes in solids shows that cavities are not required to initiate trees.

(c) Trees are initiated by charge carrier injection and extraction [31,29]. With an ac voltage, some electrons will be emitted or injected into the dielectric during the negative half cycle for a short distance, limited by the declining stress away from the point electrode. They will be drawn back into the point electrode on the following positive half cycle, and re-injected in the following cycle and so on. Some of the electrons will gain sufficient energy to cause decomposition of the polymer to lower molecular weight products and gas, resulting in the formation of a hollow channel. With dc or impulse voltages or other unidirectional voltages of some other waveshapes, the

injected charge carriers will form a space charge, making the tree initiation process more complex than that under ac fields.

At the point electrode, when the field is of the order of 10 MV/cm [3] electron or hole injection will occur by either tunneling or Schottky type thermionic emission process. In mechanism (c), some of these injected charge carriers may be trapped and some may cause ionization, and the rest may return to the electrode under ac voltages or dc voltages with suddenly changing polarity. Since the ionization energy of hydrocarbons is about 10 eV, the injected electrons may gain the energy from the field if the mean free path is around 100 Å at a field of the order of 10 MV/cm. This is unlikely to occur in polymers because in polymers the carrier mobility(μ)is less than $10^{-1}cm^2/V\cdot s$, the carrier lifetime(τ)is small and the mean free path of these materials is of the order of one to several molecular radii (5-20 Å) [21].

(d) Tree initiation and growth must involve development of easy channels for subsequent impact ionization in those channels [32]. This model, including a proposed mechanism for the development of such easy channels, is as follows: (1) Electrons and holes will be injected at high fields from the asperities on the electrode surface to the polymer. (2) The collision of an electron with a trapped hole or

free hole will release an energy of several eV. This energy, if not converted to radiative luminescence, is sufficient to break the chemical bond of the polymer chain. This process will create free volumes or mechanical cracking. (3) Once a small free volume (or an easy channel) has been created, impact ionization by electrons inside the free volume will take place, if the field in it is high enough for the electrons to gain sufficient energy to cause ionization. (4) Once ionization can occur, more free and trapped electrons and holes will be produced in and around the free volume. These charge carriers tend to break more bonds to extend the free volume (or the channel) leading to the formation of the trees.

Each of the above mechanisms requires a very high stress to provide the energy required to activate the damaging process. The idea of electron emission and injection causing the tree initiation seems most acceptable.

As the matter of fact, the C-H bonding energy is 4.28 eV; the C-C bonding energy is 3.6 eV. When the energy of the ions or electrons exceeds the bonding energy they may break the bonds making free radicals, or Hydrogen being volatile, which may diffuse out of the system, thus resulting in a change in chemical structure.

2.3 CHARGE CARRIER INJECTION FROM THE POINT ELECTRODE

In the parallel plane electrode system, charge injection from a metal electrode into a polymer dielectric has been recognized. It would be logical to presume that charge could be injected from a tip of the point electrode embedded in a polymer. Such a phenomenon was recognized in polyethylene and other polymers by (1) charge release when short-circuited, (2) laser induced liberation of remaining charge and (3) thermally-stimulated liberation of remaining charge [33].

Figure 2.2 shows the voltage dependence of injected charge current for polyethylene (PE) and polyethyleneteleph-thalate (PET) films in a point-plane electrode system. This suggests three important aspects of the charge injection characteristics of polymers: (1) Injected charge increases with increasing applied voltage. (2) Charge injection depends on the material. (3) When the electrode is positive there is still charge carrier injection.

The charge injected from the injecting contact remains inside the specimen even after the applied voltage has been removed and the specimen has been short-circuited. These charge carriers are from injected electrons being trapped in trapping centers near the point electrode. The trapped electrons if any can be optically liberated. Figures 2.3-2.4 show that the amount of trapped carriers depends on

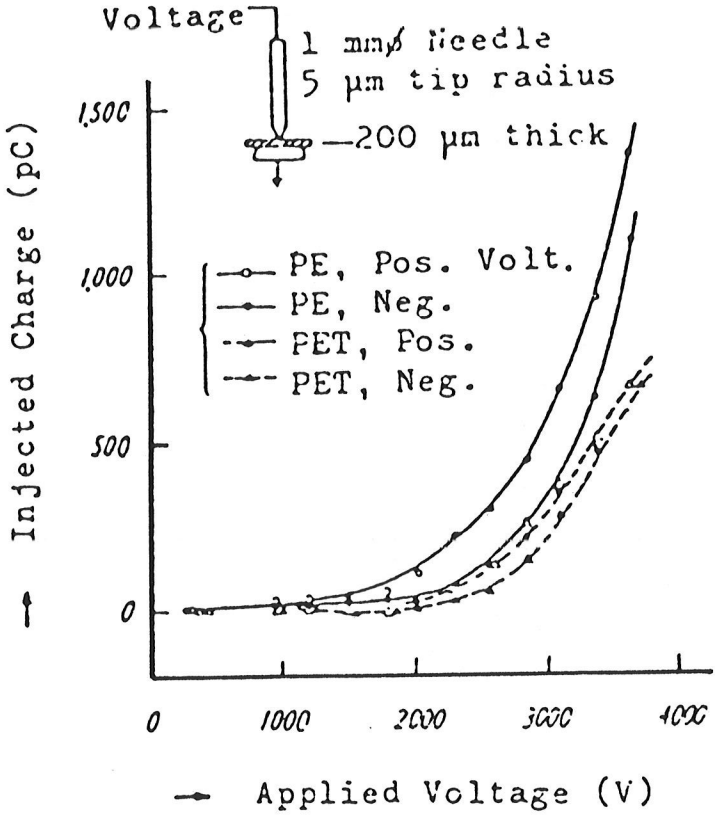

Fig. 2.2: Voltage dependence of injected charge for PE and PET films in a point-plane electrode system. (After Tanaka [33]).

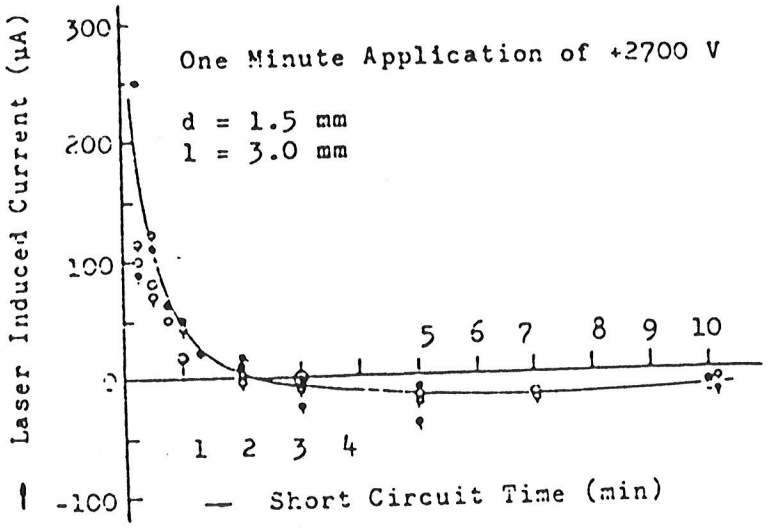

Fig. 2.3: Current due to laser-liberated charge in short-circuit condition as a function of short-circuiting time duration. (After Tanaka [33]).

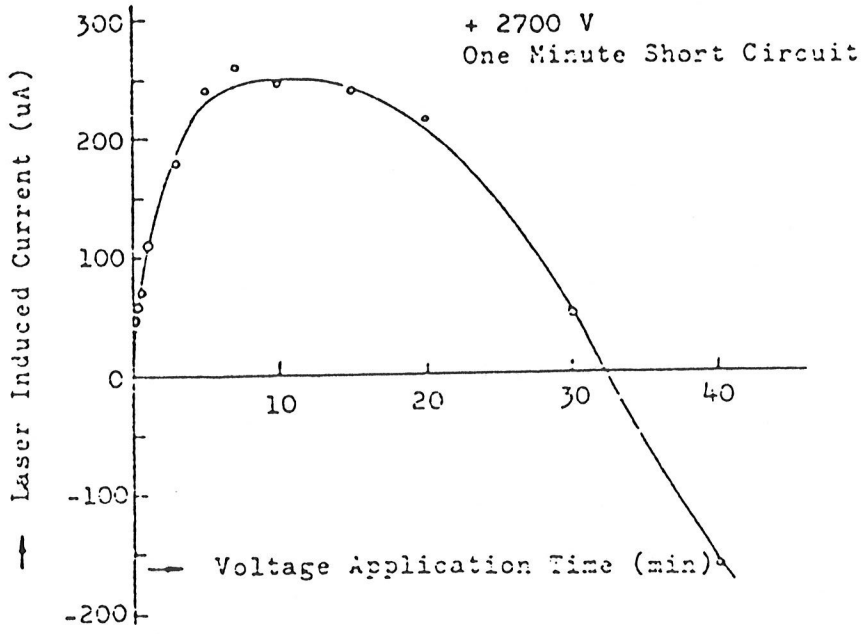

Fig. 2.4: Current due to laser-liberated charge in short-circuit condition as a function of forming time duration at room temperature. (After Tanaka [33]).

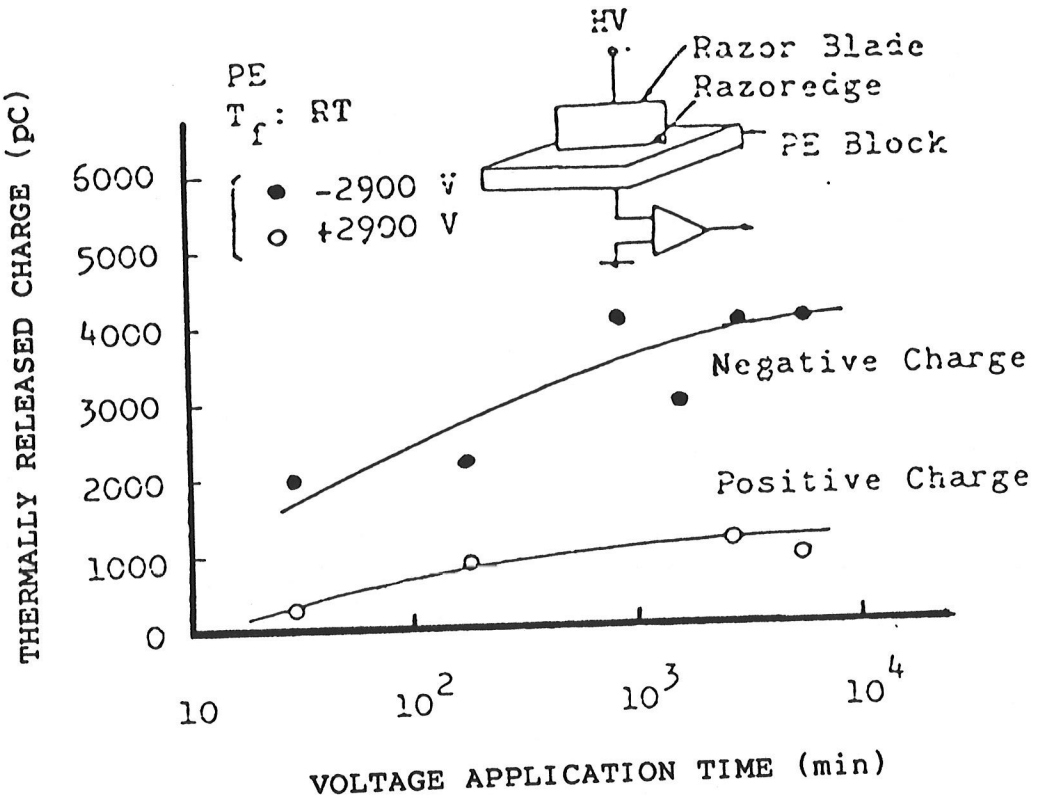

Fig. 2.5: Charge liberated by the TSC method vs. voltage application time (Charge is injected from a voltage-biased razor blade at room temperature. (After Tanaka [33]).

both the voltage application time and the short-circuit time. Trapped charge around the point tip has been estimated to be approximately 20 pC [33] from the time integral of a measured current pulse.

The thermally stimulated current (TSC) results are shown in Figure 2.5. The TSC measurements indicate that negative charge carriers are more easily trapped than positive charge carriers in polyethylene [33]. Similar results have also been reported by Buerger [34], but using a discharge detector. He divided the traps into two different kinds: (1) flat traps ($W<0.3$ eV) with a relatively small time constant influence the conduction mechanisms, and (2) shallow traps ($W\backsim 1$ eV) with a comparatively large time constant are able to build up a space charge. The traps in his model are all acceptor-like.

2.4 INTERFACIAL PHENOMENA

There are several factors controlling the charge exchange between the two materials when they subjected to the high electric field:

(a) The work functions of both the electrode metals and the dielectric materials.

(b) The existence of an insulation layer between two materials.

(c) The formation of a space charge.

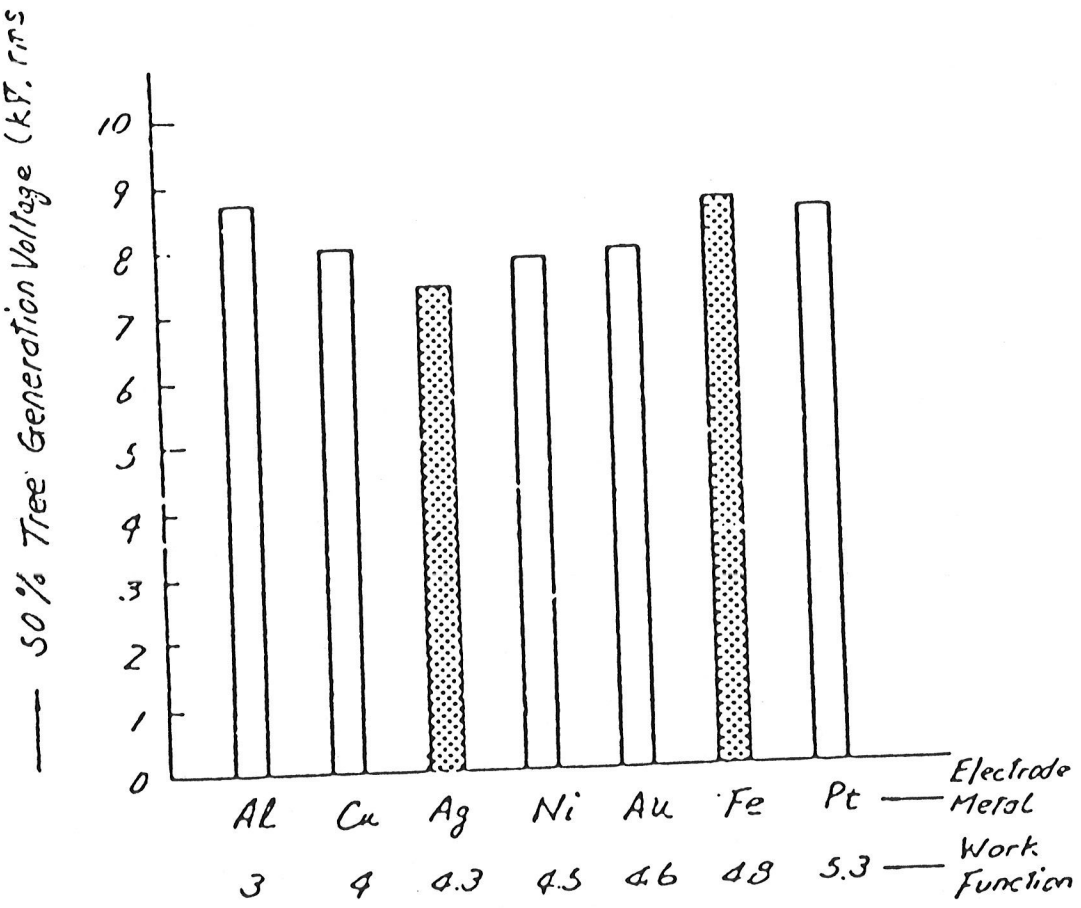

Fig. 2.6: Tree initiation voltages of various specimens with different metal point electrode. (After Tanaka [33]).

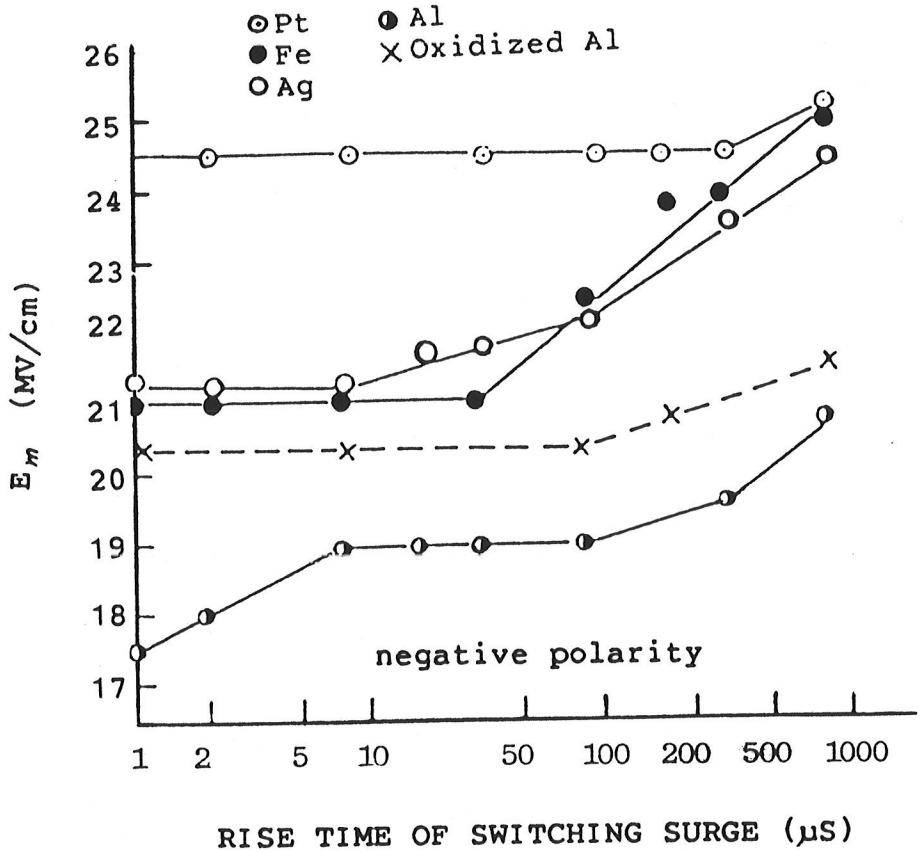

Fig. 2.7: The peak tree initiation field as a function of the rise time of the switching surge for various point electrode and Al with and without an oxide layer.
(After Yoshimura [35]).

It would be expected that if tree initiation is associated with carrier injection, a different electrode material should have a different tree initiation voltage. Figure 2.6 shows that the tree initiation voltage increases as the work function increases for Ag, Ni, Au and Fe used as electron-injecting electrodes. However, aluminum and copper do not follow the trend. It is well known that metals such as aluminum and copper are easily oxidized, forming an insulating oxide layer on the surface. This layer masks the effect of the metal work function.

Figure 2.7 shows the peak tree initiation field as a function of the rise time of the switching surge for various point electrode materials [35]. This shows that the effects of work functions are more pronounced in the fast rise speeds than in low voltage rise speeds. This may be due to a space charge accumulation around the point tip. However, Noto [35] has reported that when the point electrode is at a positive polarity the work function effects disappear.

2.5 SPACE CHARGE EFFECTS ON TREE INITIATION

Another important factor controlling the tree initiation voltage is the space charge. Without a space charge the maximum field (Ex) at the tip of the point electrode in a point-plane electrode configuration is given by [36]:

$$E_x = \frac{2V}{R \ln(1+\frac{4D}{R})}$$

where V is the applied voltage, R is the radius of the tip and D is the electrode separation.

Using this equation the field at the tip has been calculated, based on the normal tree initiation voltage, to be of the order of 30 MV/cm, which far exceeds the normal breakdown strength of 6.5 MV/cm for polyethylene [37], and also for other materials. This discrepancy may be attributed to the effects of space charges. Kosaki et.al.[37] have calculated the potential and field distribution at the tip of the point electrode taking into account of the injected homospace charge. Their results are shown in Fig. 2.8. When the applied dc voltage is 40 kV, the space charge is estimated to have expanded to a distance of about 10 um from the tip with a uniform charge density of about 10 C/cm^3 and the field at the tip is lowered to zero. However, at the edge of the space charge region, the maximum field is about 9 MV/cm. It has been found [33,37] that the pattern of a tree always follows the initial tree length, which is defined as the distance from the tip to the point from which the first tree branch begins. It is possible that the initial tree length is associated with the distance that the injected electrons can reach. Since the space charge is

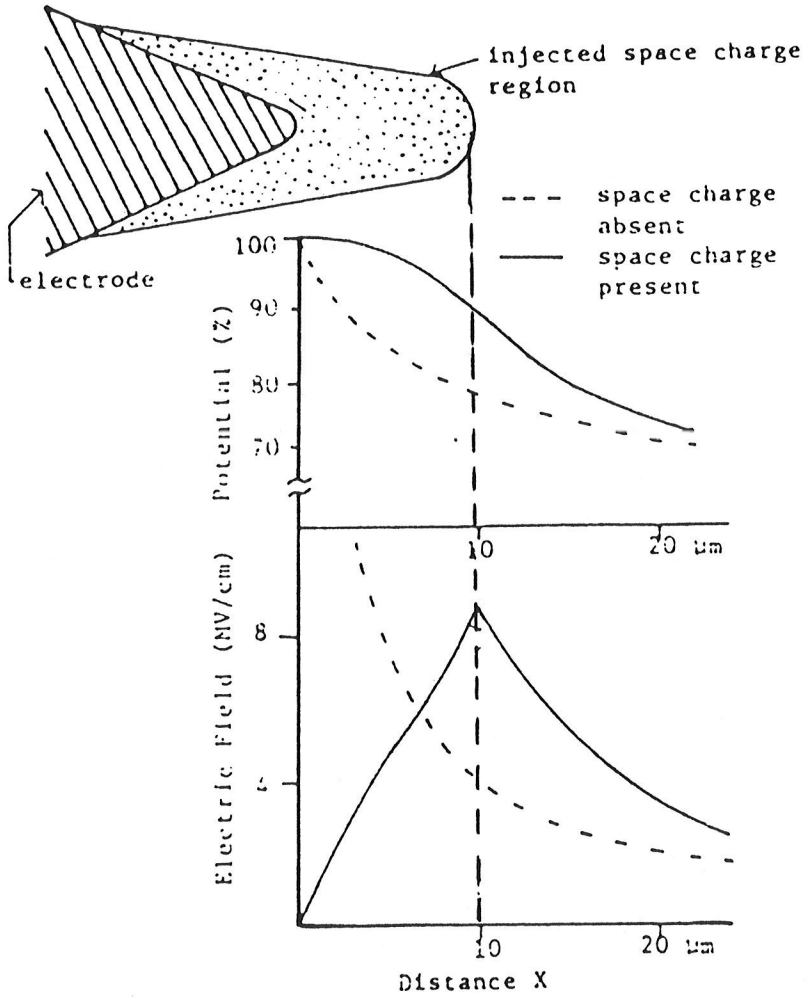

Fig. 2.8: Potential and field distribution at point tip with injected space charge. (After Kosaki [37]).

mainly due to injected carriers trapped in the localized states (trapping centers), the formation of the space charge is controlled by the trapping parameters. Obviously, the formation of the space charge is responsible for the polarity effect on the tree initiation voltage, as shown in Fig. 2.9, and Tables 2.2 and 2.3

Time is required for the formation of space charge and time is also required for its decay. An effective space charge density may need a few hundred microseconds to form[37,38], and may need about 10 ms to decay to a insignificant value after the removal of the stressing voltage. Because of the dependence of the formation of the space charge on time, the tree initiation voltage is expected to depend on the rise time of the applied stressing voltage [39] as shown in Fig. 2.9 and Table 2.2 and 2.3.

2.6 THE EFFECTS OF AN OXIDE LAYER ON THE INJECTING ELECTRODE SURFACE

So far very little work have been reported on the effects of an oxide layer on the tree initiation voltage. Yoshimura et al. [35] have studied the effect of an oxide layer on a metallic point electrode on the treeing properties under switch surge. Figure 2.7 show that an Alumina point electrode with an oxide layer gives a higher tree initiation voltage than that without an oxide layer when point electrode is negative. But this effect becomes less when the

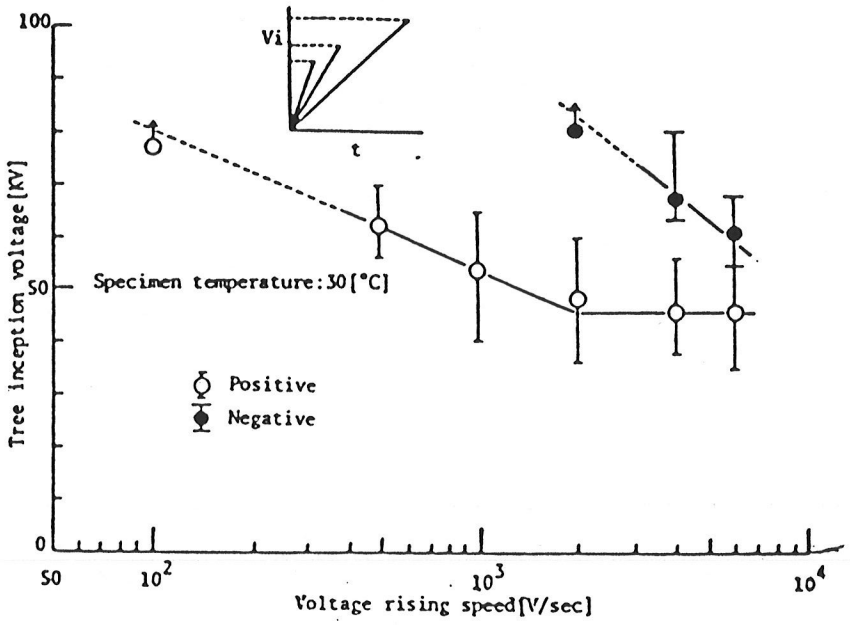

Fig. 2.9: Inception voltage and dc tree as a function of voltage-rise speed.
(After Ieda [39]).

Table 2.2

The Mean 50% Tree Initiation Voltage in kV

Material	Needle - Plate			Needle - Needle		
	dc		ac	dc**	ac	
	+ Needle	- Needle	Symm		Symm	Asymm
PE	37.0 (55.5)*	54.0 (44.0)*	5.9	77.0	11.0	10.0
XLPE	46.0	40.0	6.1	-	10.7	9.6
PE + A+	49.5	48.6	17.0	-	37.0	-

\+ Acetophenone content: 1%.
* Slow rise of the applied dc voltage.
** All trees initiated at negative needles.

Table 2.3

The Mean Breakdown Voltage in kV++

Material	Needle-Plate			Needle-Needle	
	dc		ac	dc	ac
	+ Needle	- Needle	Symm		Symm
PE	39.0	100.0	33.0*	100.0	56.5
XLPE	78.0	96.0	33.0**	>150.0	59.4
PE + A+	55.0	64.0	40.0***	108.0	62.8

\+ Acetophenone content: 1%.
++ Each value is the average value of 14-20 samples.
* 16 out of 16 samples broke down at the positive half cycle.
** 14 out of 17 samples broke down at the positive half cycle.
*** 14 out of 16 samples broke down at the positive half cycle.

(After Kao [32]).

rise time of the switching surge is over 100 us. They attributed this phenomena to the space charge accumulated in the polyethylene surrounding the point tip. The space charge relieves the electric field around the point tip and therefore a higher voltage to initiate the tree is required, especially for a non-oxide point electrode.

2.7 THE EFFECTS OF ADDITIVES ON TREE INITIATION

After many years of research on polymeric insulation failure, it is generally realized that it is not possible to produce a perfect polymeric insulation system, since cavities, contamination, mechanical stresses etc. are always present. Therefore scientists and technologists have to try to live with the presence of such defects. Obviously, the first idea to solve this problem is to increase the threshold voltage for the onset of electrical trees. Since 1974 investigators [7] have found that additives in a polymer change the properties of the polymer. In the past ten years, hundreds of different additives had been tested for the suppression of initiation and the growth of electrical trees. It is well known that some additives such as dodecanol, acetophenone etc. do increase the tree initiation voltage under certain conditions. Some important experimental results on the effects of additives are summarized as follows:

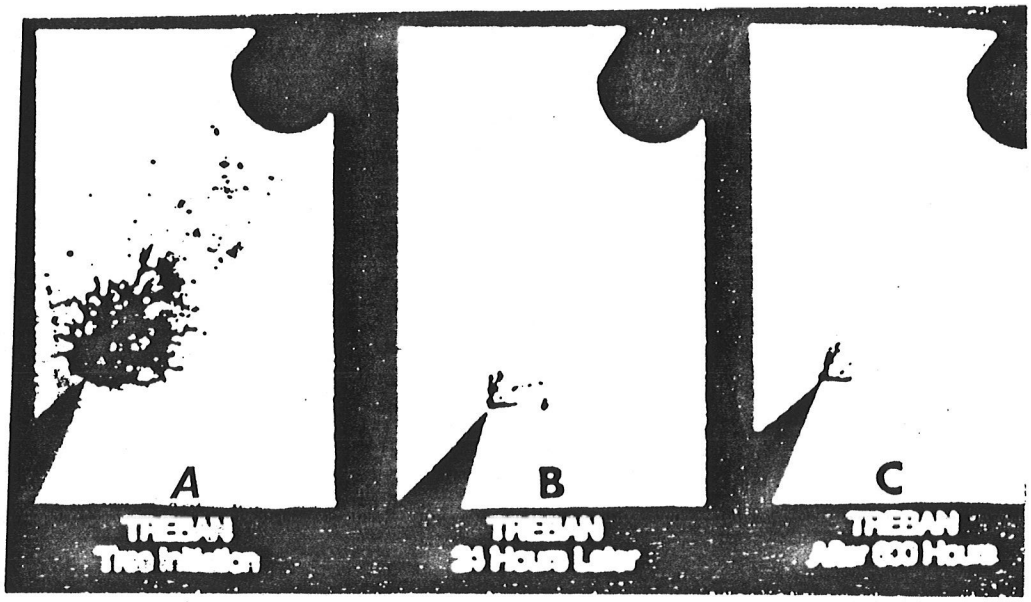

Fig. 2.10: The effects of additive on electrical tree growth. (A) Tree initiation - 40 kV, 2 sec. (B)After 24 hrs.(C)After 800 hrs. at 12 kv. (After McMahon [7]).

Figure 2.10 shows a series of pictures of a polyethylene specimen with a point-plane electrode containing dodecanol. Figure 2.10A shows the tree that was formed after the application of 35 kV for 2 sec; Figure 2.10B shows the tree after the specimen has been short-circuited for 24 hours, it appears much smaller; and Figure 2.10C shows the tree exposure to 12 kV for 800 hours, for which the tree had not grown. Such tests have been run for 2 1/2 years without failure. This experiment indicated dodecanol to be an excellent additive which could prevent electrical trees in cable. Even after a tree is formed, which might occur in cable in service due to lighting, the indications are that the dodecanol would protect the cable dielectric from failure [7].

Table 2.2 and 2.3 shows the mean tree initiation voltage and the mean breakdown voltage for pure polyethylene and polyethylene with added acetophenone [32]. The additives increase both the tree initiation and breakdown voltages under ac and dc stressing voltage with the point electrode positive. However, the additives gave a lower tree initiation voltage and breakdown voltage if the point electrode is negative, indicating the importance of the space charge effects.

Some other experimental results show that impurities added in polymers can increase the electrical tree initiation voltage [40].

The above experimental results suggest that additives inhibit the tree growth even after the tree has been formed. The additives may act as a voltage stabilizer and the additives can also increase the tree initiation voltage and the breakdown voltage under some electrical conditions.

Some possible mechanisms responsible for the inhibition of the initiation and the growth of the trees are summarized as follows:

(a) The additive can migrate within the polyethylene matrix and is free to move and enter the tree channels once the tree has initiated. The growth of a tree is inhibited by grading the electric field. This mechanism was first suggested by McMahon [7] based on his experimental results and the fact that it is not possible to prevent the trees from initiating particularly when the insulation systems are subjected to high voltage impulses from the lighting or switching surges. In this mechanism, the impurities do little to raise the tree inception voltage, but do inhibit the growth of a tree once it has been initiated. This mechanism is not consistent with the experimental results found by other investigators, which is that the additives can increase the tree initiation voltage.

(b) The additives can inhibit the tree by a chemical reaction [3,40]. The ionization potential of the hydrocarbons may be associated with their inhibition ability. The

difficulty encountered with this mechanism is that the energy required to break the chemical bonds is much less than 10 eV, while the ionization potential of some good additive components exceeds 10 eV.

(c) The tree inhibition is due to the field grading mechanism [41]. The additives behaves as a field-dependent conducting material. The higher the electric field, the larger is the conductivity. There are two mechanisms responsible for the field-dependant conductivity: (1) Field-enhanced dissociation, that is, the rate of dissociation of weak electrolytes increases with increasing electrical field, which products a higher conductivity in the high field region. (2) Field-enhanced ionization, that is, the rate of ionization of the low ionization potential additives increase with increasing electrical field, which products also a higher conductivity in the high field region.

This stress-grading mechanism is not consistent with other features related to the breakdown phenomena. For example, the additives under dc conditions with the point negative do not increase the tree initiation voltage.

(d) The increasing of the voltage for an electrical tree by additives may be due to the introduction of shallow traps to reduce the energy of hot electrons so as to reduce the energy released due to trapping and recombination [21]. In

this case, the bond breaking may involve a multi-hot electron bombardment.

Chapter III

THE INFLUENCE OF AN OXIDE LAYER AT THE METAL-POLYMER INTERFACE ON ELECTRICAL TREEING PROPERTIES OF POLYETHYLENE

The effects of electrode materials on the tree initiation voltage with ac stressing voltages and switching surge conditions have been reported [33,35]. For a point-plane electrode configuration it has been found that the tree initiation voltage depends on the work function of the metallic point electrode if the point is negative in polarity, but such a dependence disappears if the point is positive in polarity [39]. However, there is no reason to doubt that hole injection is as feasible as electron injection in polymers. In fact, positive charge carrier injection in polyethylene has been reported [33]. It is possible that holes are injected not directly to the valence band but rather to the localized states in the energy gap to form trapped hole space charges because of the high and wide potential barrier near the anode. In this case the hole injection efficiency may depend more on the trap distribution near the Fermi level than on the work function of the metal itself [32]. On the basis of light emission experi-

ments, Kosaki et al. [42] have reported that there are holes injected from the point anode to polyethylene. In order to examine how important electron and hole injection is to the electrical treeing properties, we have carried out a study of the influence of an oxide layer at the interface between the metallic point and the polymer on these properties.

3.1 EXPERIMENTAL DETAILS

The polymer used for this investigation was polyethylene. All samples were cut into the form of a block of 6 mm x 10 mm x 50 mm in size. The size of the polyethylene specimens and the point-plane separation are shown in Fig. 3.1. Two metals for the point electrodes were used: aluminum and iron. The point was produced by mechanically polishing a pure aluminum or pure iron wire of diameter of 0.5 mm to form a point shape tip, the radius of curvature of the tip of both the aluminum and iron points being around 4μm. The purity of both the aluminum wire and iron wire is 0.9999. The point was cleaned with methylbenzene and acetone, then dried in a vacuum oven. Prior to the insertion of these points into polyethylene blocks, some of the point electrodes were oxidized inside a quartz tube which was placed inside a diffusion furnace at 560 °C for about four hours, through which oxygen gas was flowing. The thickness of the oxide layer was about 10 μm. The polymer block was heated to 180 °C and kept at this temperature for

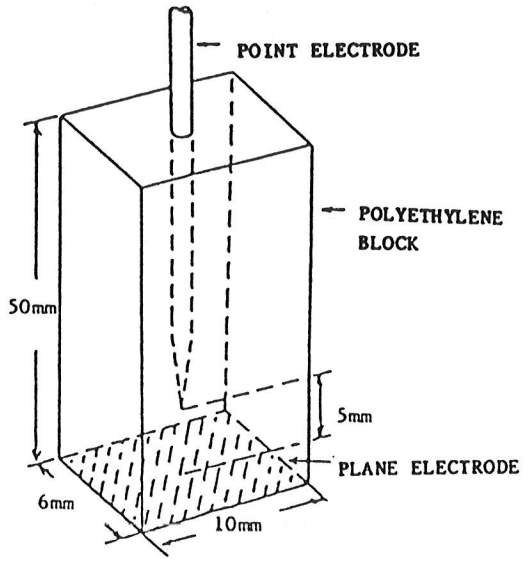

Fig. 3.1: Point-plane electrode configuration.

about 15 min to enable the insertion of the points. After the insertion the specimen was slowly cooled down to room temperature.

For this investigation we used mainly unidirectional triangular pulse voltages with a rise time varying from 5 s to 40 s, a duration of 2 min. and a pause time of 1 min. between pulses as shown in Fig. 3.2. The rise time was much shorter than the decay time. The decay times are very long so that there are no short circuit effects. All experiments were performed with the specimens immersed in transformer oil at room temperature. For each predetermined stressing voltage ten identical specimens were used and these specimens were examined under a microscope of magnification 200. The stressing time was 10 pulses at one stressing voltage, and the voltage was raised in 5 kV per step until the appearance of trees. We also used single impulse, unidirectional rectangular pulses and ac voltage to study the effects of the oxide layer on electrical tree properties. The 50% tree initiation voltage is defined as the voltage at which 50% of the total number of specimens contain trees with a tree penetration length equal to or larger than 10 μm.

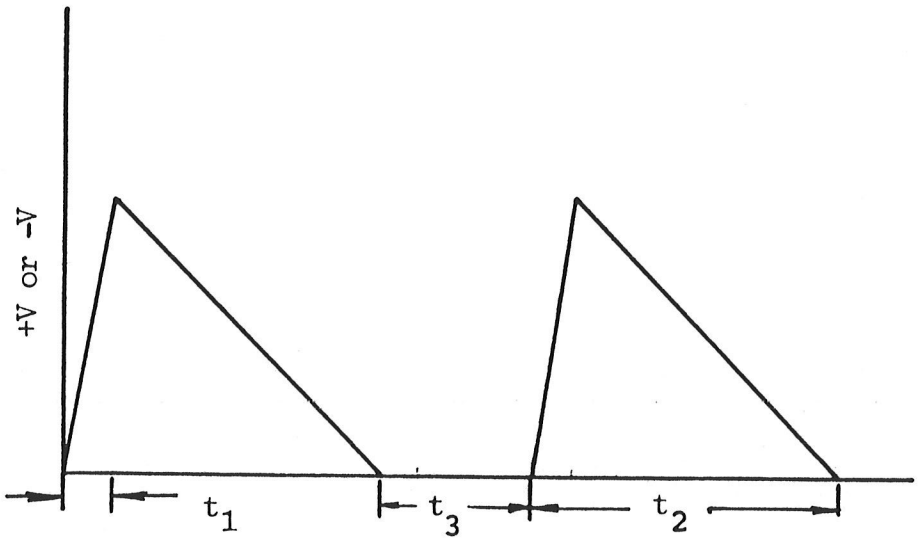

Fig. 3.2: The rise time, duration and pause time of unidirectional triangular pause voltage.

THREE VOLTAGE RISE TIME

t_1(S)	t_2(min)	t_3(min)
5	2	2
20	2	2
40	2	2

3.2 RESULTS AND DISCUSSION

Figure 3.3 shows the effects of the point metal and the polarity of the applied voltage at the point. Figure 3.4-3.5 show the effects of an oxide layer at the metal-polymer interface on the tree initiation voltage in polyethylene when the point is at the positive and negative polarities, respectively. It can be seen that the carrier injection from both the cathode and the anode plays the decisive role in the formation of trees.

3.2.1 Work Function Effects

The tree initiation voltage Vt depends roughly on the work function of the point electrode material. The work functions of pure aluminum and pure iron are about 3.0 eV and 4.8 eV, respectively. There is a correlation between Vt and the work function when the point is negative in polarity, but such a dependence disappears when the point is positive in polarity. A similar finding involving other metals has also been reported by other investigators [35,39]. To explain this phenomenon we should consider the charge carrier injection process.

The electron injection from the metal to the polymer may mainly involve tunneling or thermionic emission. Thus the electrons injection efficiency may be loosely related to the work function of the electrode material.

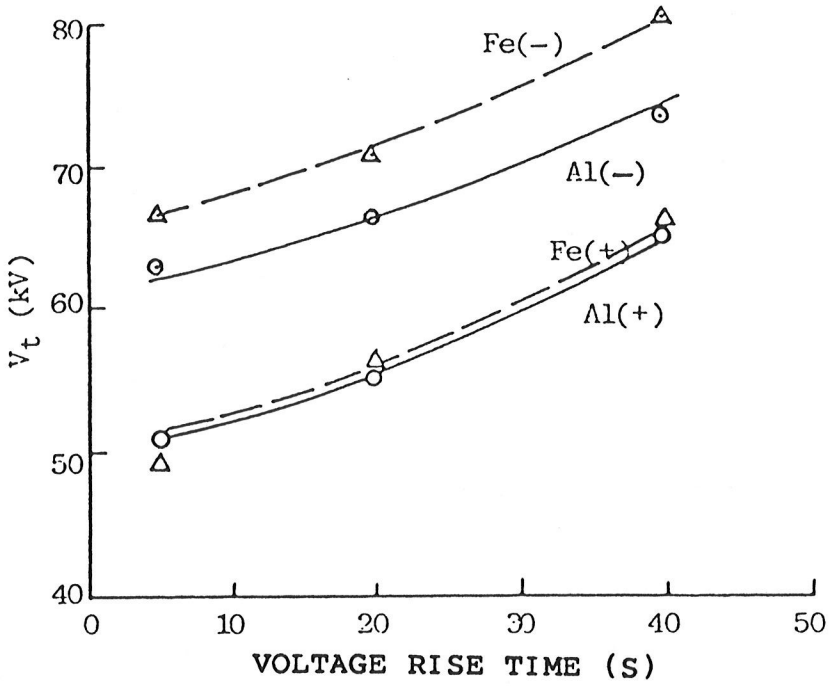

Fig. 3.3: The tree initiation voltage Vt as a function of the rise time of the stressing voltage. (Triangular waveshape unidirectional voltage) ○ Al(+), ⊙ Al(−), △ Fe(+) and ▲ Fe(−) denote the point metal Al and Fe and the polarity of the voltage at the point electrode (+) and (−).

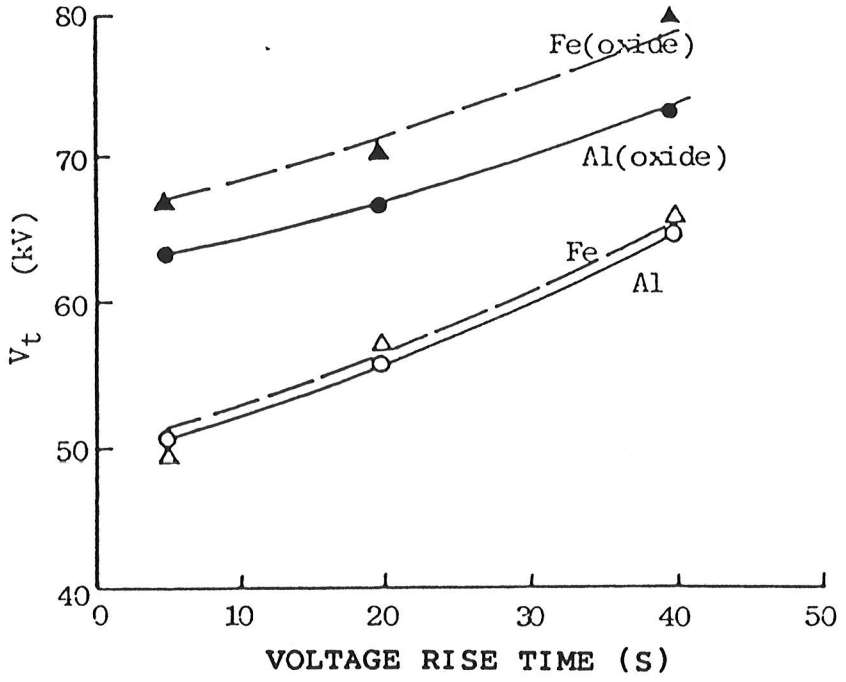

Fig. 3.4: The effect of the oxide layer on the tree initiation voltage Vt with the point electrode at the positive polarity.
○ Al(without oxide), ● Al(with oxide)
△ Fe(without oxide), ▲ Fe(with oxide).

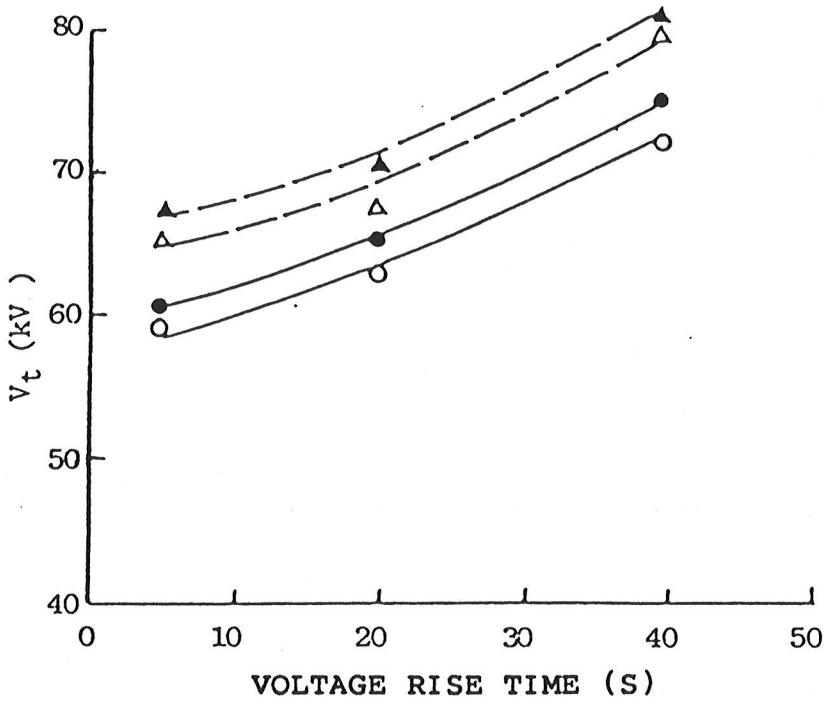

Fig. 3.5: The effect of the oxide layer on the tree initiation voltage Vt with the point electrode at the negative polarity.
O Al(without oxide), ● Al(with oxide)
△ Fe(without oxide), ▲ Fe(with oxide).

However, holes may be directly injected to localized states near the Fermi level to form trapped holes and thus the injection efficiency is not so sensitive to the work function of the point electrode material, but it may depend on the concentration of the localized states near the hole injecting contact. A similar finding involving other metals has also been reported by other investigators.

3.2.2 Behaviours of Injected Charge Carriers

The formation of an electrical tree is associated with charge carriers injection from the point electrode. The injected carriers produce a homo-space charge which tends to suppress further carrier injection. This process tends to increase Vt, since the injected carriers are immediately trapped or recombined with particles of opposite charge, or in trapping and recombination centers. The energy released from the trapping or recombination will be partly converted to energy for breaking bonds and creating low-density channels or domains to favour subsequent electron impact ionization. This process tends to reduce Vt. It is possible that the rate of the former process increases and the rate of the latter process decreases with increasing rise time of the applied voltage. These two processes compete with each other, thus resulting in the rise time dependence of Vt.

Regardless of whether the point is negative or positive, the final discharge process is due to the avalanche of electron impact ionization in the low density regions or channels. The initial electrons come from the electron emission if the point is the cathode, but come from a different source related to the hole injection if the point electrode is the anode [21]. The holes injected into traps will form a homo-space charge in a manner similar to electron injection from the point cathode. For a short rise time, the energy gained by electrons moving in a converging field near the positive point tip is more than that gained in a divergent field near the negative point tip. Furthermore, electron injection is more efficient than hole injection for the formation of homo-space charge for a point plane electrode configuration in polyethylene. This is why the negative point gives a higher value of Vt than the positive point.

However if the rise time is long, another mechanism may become more effective, such as an increase of the trapped hole concentration which may reduce the effectiveness of electron impact ionization in the low-density regions. This mechanism may make the trend of the polarity dependence reverse. In fact, we have observed such a reversae in the effect of the point polarity on Vt under dc voltage conditions. In this case the point plane separation used was 1.5 mm. The results are shown in Table 3.1.

Table 3.1 The effect of the needle electrode polarity on the dc tree initiation voltage

Needle Polarity	V_t (kV)	
	Fast Rise*	Slow Rise**
Positive	37.0	55.5
Negative	54.0	44.0

* Rise time was 2 kV/s until a predetermined stressing voltage was reached. The stressing time was one hour.

** Rise time was 2 kV/s up to 50% of the predetermined stressing voltage and then with the increase in steps at 2 kV per step every minute up to the predetermined voltage. The stressing time was one hour.

Table 3.2 The effect of the oxide layer at the aluminum needle-polyethylene interface on the tree initiation voltage under unidirectional rectangular pulse conditions

Needle Polarity	V_t (kV)	
	With Oxide	Without Oxide
Positive	35.0	28.3
Negative	24.2	22.3

The needle-plate separation was 2 mm and the stressing time was 100 pulses.

Noto et al. [38] have reported that Vt, under impulse voltage conditions, is lower than that under dc voltage conditions (with a short rise time). Thus, based on the aforementioned two competitive process, it can be imagined that there should be a rise time for a given point electrode material and a given polymer, at which the polarity dependence disappears.

It is likely that a trapped hole injected from the point anode may transport from one gap state to another by either a tunneling or hopping process, and may have to travel a certain distance before it has a chance to recombine with a free or trapped electron to result in dissociation recombination. So the injected holes do not form a high concentration space charge region. This may be the reason why the tree penetration length is longer when the point is positive than when it is negative as shown in Fig. 3.6. It is interesting to note that the oxide layer on the point surface does not affect the pattern of the tree though it significantly affects the value of Vt.

3.2.3 The Oxide Layer Effect

So far as we have observed, the oxide layer at the injecting contact polymer interface increases Vt, and this effect is more pronounced when the point is positive than when it is negative as shown in Fig. 3.4 and Fig. 3.5. This

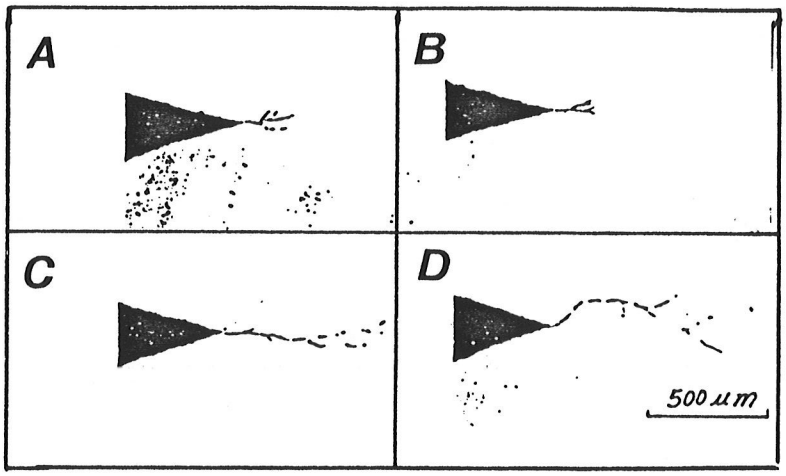

Fig. 3.6: Photographs of trees.
A. Al(without oxide) negative point, V=62 kV
B. Al(with oxide) negative point, V=65 kV
C. Al(without oxide) positive point, V=56 kV
D. Al(with oxide) positive point, V=67 kV

indicates that traps in polyethylene are acceptor-like. When the point electrode is negative in polarity, the injected electrons will form a strong space charge region that modify the electric field, and restrain the injection process which means the oxide layer has little effect on Vt.

But for the aluminum point at an negative polarity with the point-plane separation 5 mm, the tree initiation voltages measured with a single 1.5/50 μs impulse were 108 kV and 90 kV for the point with and without an oxide layer, respectively. The reason is that there is no time to form the space charge region with such a fast voltage rise time, so the oxide layer effect on Vt appears when the point electrode is negative.

For the injected positive charge carrier, Vt will depend on the number of injected carriers. An oxide on the point electrode will suppress considerably the charge carrier injection, so in this case, the injecting electrode with an oxide layer gives a higher Vt than that without oxide.

We have also performed the experiment with unidirectional rectangular pulses with a rise time of 0.03 s, a duration of 4 s and a short circuit time of 1 s between pulses. The results are shown in Table 3.2. In this case it is likely that the tree occurs during the short circuit time between pulses. This may be why the tree initiation voltage is much lower than that under the unidirectional triangular

pulse; in the latter case, the pulse decay time is so long that the short-circuit effect is eliminated. The data imply also that the homo-space charge created during the electrical stressing may create a field toward the point electrode at the time of short circuiting, which is much higher than the applied stressing field [43]. For the negative point without oxide case, the homo-space charge is much more easily formed than in the other case; this may be the reason why the negative point without oxide has the lowest tree initiation voltage.

The polarity effect in the tree initiation caused by a short circuit seems to be opposite to that caused by the dc stressing. The reason is that the pronounced space charge at the negative point electrode causes strong alleviation of the electric field and gives rise to an increase in the dc tree initiation voltage, but such a pronounced space charge after short circuit produces a strong field toward the point electrode, thus causing the formation of trees Consequently, there is no contradiction about the polarity effect in both cases.

In the ac case, the tree initiation voltages were 8 kV and 6 kV for iron point with and without an oxide layer, respectively, the point-plane separation in this case being 2 mm. Base on the above results, the oxide layer may be considered to be a barrier to suppress the direct communica-

tion between the carrier injecting contact and the polymer, thus reducing the efficiency of carrier injection into the polymer. Further work using different experimental approaches is necessary in order to study the physics of this effect. The present results indicate that an interfacial oxide layer is beneficial to the practical polymeric insulation systems.

3.3 CONCLUSIONS

(1) The interfacial oxide layer can be considered to be a barrier suppressing direct communication between the carrier injection contact and the polymer, thus reducing the efficiency of carrier injection into polymer.

(2) An interfacial oxide layer is beneficial to practical polymeric insulation systems.

(3) The oxide layer has no effects on the pattern of the trees. This implies that the tree pattern depends mainly on the type of carriers rather than the number of carriers injected from the injecting contact.

Chapter IV

COMPUTER SIMULATION OF DISCHARGE PATTERNS

The discharge patterns (tree) for the negative point electrode are quite different from those for the positive point electrode. The difference in fractal behaviour arises from a simple reversal of the polarity of the point electrode. When the point electrode is negatively biased, the discharge pattern is highly ramified, indicating that the process has a strong stochastic nature. This contrasts with the behavior when the point electrode is positively biased, in this case there is a strong tendency for the discharge to grow on the points where the electric field is the greatest. This reduces the tendency to ramify, indicating that the process is a deterministic one in this case.

In this Chapter we present our computer simulation of a theoretical model for the field dependence of the breakdown probability. This simulation may help to understand the phenomena in the space-charge region surrounding the discharge patterns.

4.1 STOCHASTIC MODEL

Initial theoretical investigations by Pietronero et.al.[44,45] were based upon radially symmetric two-dimensional discharge patterns. The fractal object was characterized by a non-integer power law dependence between the 'mass'(N) and the radius(R):

$$N \approx R^{D} \qquad (1)$$

where D is the Hausdorff or fractal dimension [4]. The stochastic model introduced by these authors [44,45] was based upon two simple rules:

(1) The discharge pattern is equipotential and connected and

(2) The probability Pj to add the segment j connected to the pattern is proportional to a power of the local electric field Ej

Arguments justifying these assumptions are described in Ref.[44] and are based upon the physical reasoning of field fluctuations in real dynamical systems. The stochastic nature of the breakdown process and branching of the tree, which is its precursor, is attributed to these fluctuations. Pietronero et.al.[5] characterized the electrical field dependence of the branching probability by a power law as follows :

$$P_j \approx E_j^{\eta} \qquad (2)$$

where n is an empirical parameter and E is the local electric field. We have adopted this same form of Eq(2) for P in our computer simulation.

The above rules provide us the solution of the Laplace equation with the appropriate boundary conditions defined by the growing equipotential pattern. We assume ϕ =0 along the discharge pattern and ϕ =1 outside a local electric field. The probability field for the addition of a segment is therefore related to the values of the potential in all the points surrounding the already available pattern. To determine it, the discrete Laplace equation

$$\frac{1}{4}\phi_{K,j} = \phi_{K,j+1} + \phi_{K,j-1} + \phi_{K+1,j} + \phi_{K-1,j} \quad (3)$$

is solved by iterations with the above specified boundary condition.

The basic idea of this model is that the discharge pattern does not only grow at the point of maximum local field but also grow at the point where the probability of growing is also the highest. This is one of the reason why for discharge we always obtain a stochastic pattern instead of a straight line.

4.2 COMPUTER SIMULATION

The computer simulations were conducted upon a rectangular grid; the grid contained a point source together with appropriate boundary conditions. In our case the grid modeled a point above a conducting ground plane. At each time step the discharge pattern was allowed to grow by the addition of one bond, constrained by the model assumptions and in accordance with Eq.(2). The discharge pattern including the new bond were field values. These field values were in turn employed in the calculation of the new probabilities, in a iterative manner.

4.3 DISCUSSION

Experimental results for electrical discharge patterns in our polyethylene samples are shown in Fig 4.1. One can immediately note the difference in the fractal behavior of the discharge pattern when the polarity is reversed. Figure 4.1A illustrates the discharge when the point acts as the cathodes. In this case the pattern is highly ramified indicating that the discharge is not only field dependent but also governed by a stochastic process. Figure 4.1B illustrates the discharge when the point acts as the anode. In this case the pattern resembles a low dimensional random walker [4]. The suppression of the degree of ramification

(A)

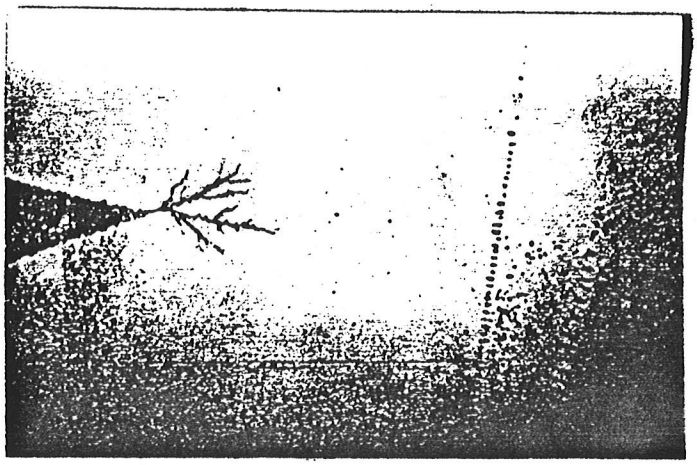

(B)

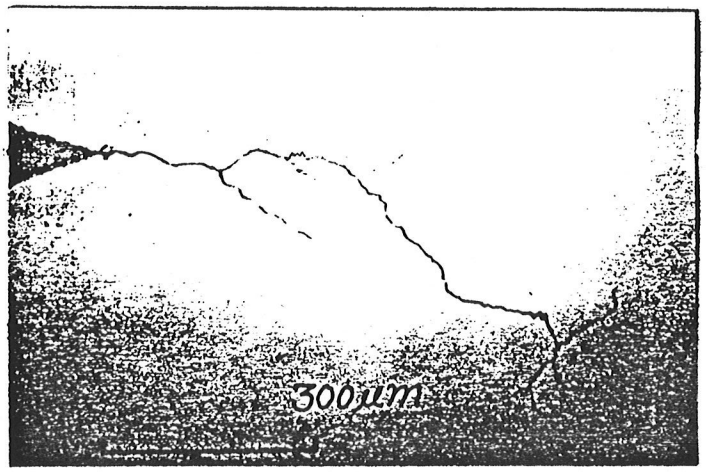

Fig. 4.1: Experimental discharge pattern
(A) when the point acts as the cathode
(B) when the point acts as the anode.

(A)

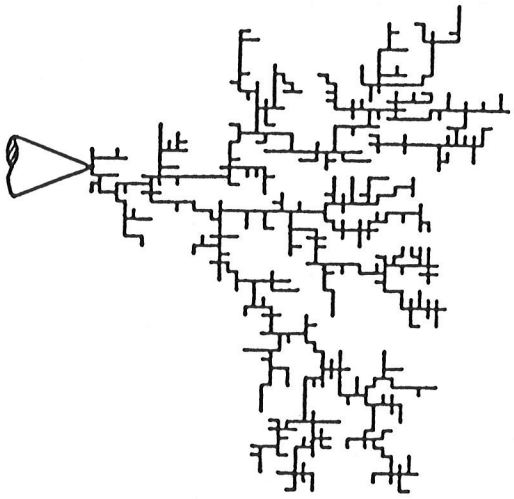

(B)

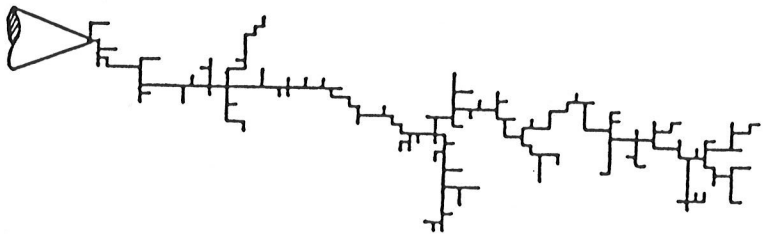

Fig.4.2: Simulated discharge pattern (A) when the field dependence of branching probability η =0.50 and (B) when η=1.5.

suggest a more deterministic field dependent process. Computer simulations based upon the stochastic model for dielectric breakdown indicate a similar structure when the parameter(η) in Eg.(2) for the field dependence of the branching probability is varied. Figure 4.2A illustrates the simulated discharge pattern when η=0.5 ; this weak field dependence of the probability accentuates the stochastic nature of the breakdown. Figure 4.2B illustrates the simulated breakdown pattern when η=1.5 ; in this case the pronounced field dependence of the probability is manifested in the deterministic nature of the breakdown. That is, there is an overwhelming tendency for the discharge to grow at the point where the electric field is the highest, suggesting that the discharge will proceed along an electric field line, indicative of deterministic behavior. Comparing Fig. 4.1 and Fig. 4.2, one immediately notes a high correlation between the point polarity and the field dependence of the probability (η). The field dependence (η) is polarity dependent since the discharge mechanism is polarity-dependent. This correlation maps directly into a correspondence between the physical phenomenon and the fractal dimensions. The physical phenomenon is that of charge transport and the influence of the associated space-charge regions. For a point cathode, it is believed that electrons are easily trapped and form a homo-space charge region, which modifies the electric field, so the

discharge pattern appeares more stochastic. For a point anode, the number of injected positive charge carriers is less and the energy gained by electrons moving in a converging field near the positive needle tip is more than that gained in a divergent field near the negative point tip. These are the reasons why the discharge pattern in this case is more deterministic. This phenomenon is consistent with the experiment results discussed in Chapter III.

So far, in the computer simulation of discharge patterns Laplace's equation is still used to solve the electric field, which is an approximation. Further work will take the space-charge and time effects into account.

Chapter V

THE EFFECTS OF INCORPORATED IMPURITIES ON THE BREAKDOWN PROPERTIES OF POLYETHYLENE

Foreign elements incorporated in a material will cause changes in both its structure and composition, which may lead to novel properties. For instance, group III and group V elements doped into a group IV semiconductor, such as Si, will convert the semiconductor material to a p-type or n-type semiconductor, which plays a vital role in today's electronics industries. The same impact may happen in polymers. Over the past ten years, investigators have successfully changed semiconducting polymers into p-type or n-type semiconducting polymers, and produced p-n junctions in polymers [6]. From an insulation point of view, the impurity incorporated should also affect the breakdown properties of the polymer. However, little has been reported on the effects of incorporated impurities on the breakdown strength of polyethylene. In this Chapter we shall report some new results about the effects of incorporated impurities on breakdown properties of the polyethylene.

5.1 EXPERIMENTAL DETAILS

The specimens used in this investigation were prepared using a plasma implantation technique. The glow discharge reactor shown in Fig. 5.1 consists of two parallel plate electrodes connected to a current-regulated radio-frequency (rf) power supply of frequency 13.6 MHz. The electrodes are aluminum discs covered with a polyethylene film of 15 cm in diameter and 1 cm in thickness with round edges, the electrode separation being 5 cm.

Glass substrates already covered with a pure polymer film were placed on the bottom electrode. There was always heat-input to the substrates from the glow discharge; this heat, however, was not sufficient to raise the substrate temperature to a temperature close to the melting point of the polymer film. Thermocouples and a resistance heater were embedded beneath the bottom electrode to monitor and control the substrate temperature.

The first steps in the plasma implantation process were to evacuate the system to about 10^{-6} Torr, establish a pressure of a desired gas mixture (about 0.1 Torr) which contains the foreign elements, and then raise the substrate temperature to a temperature of about 80-90% of the melting point temperature of the polymer film. After the completion of these steps the rf power supply and negative dc bias applied to the bottom electrode were turned on to start the

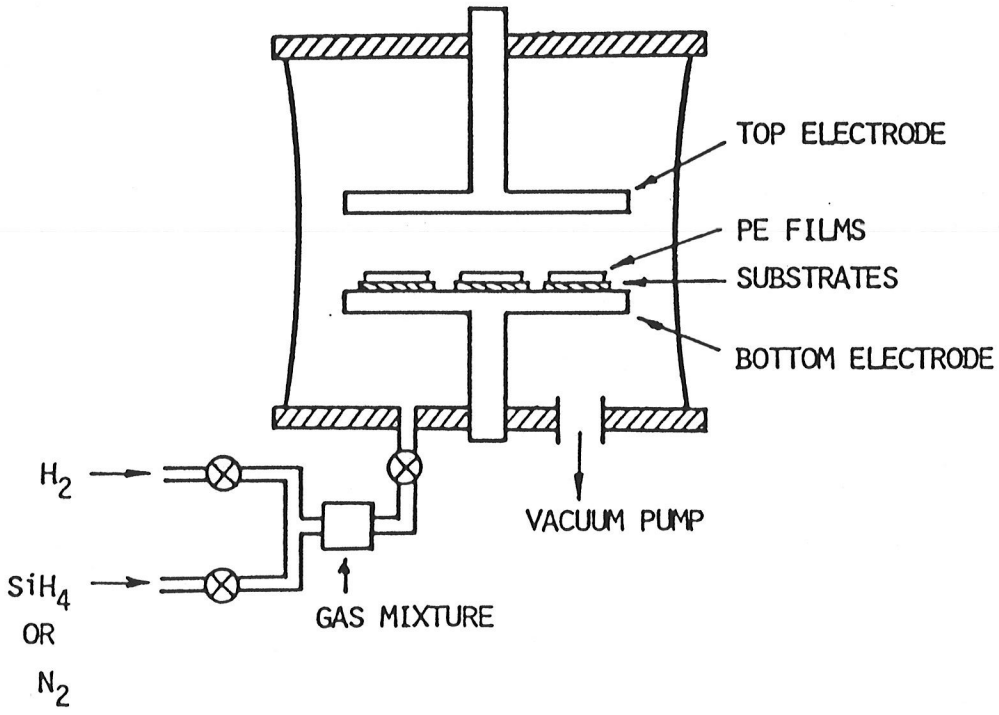

Fig. 5.1: Simplified schematic diagram of the plasma implantation system.

plasma implantation process. The rate of foreign element implantation and the uniformity of the foreign element distribution in the film depend on the gas mixture ratio, such as the SiH_4/H_2 ratio in which SiH_4 and H_2 denote the volume concentrations of the gas containing Si as the foreign elements and the diluting gas H_2, respectively; the gas pressure in the system; the gas flow rate; the rf power; the negative bias voltage; and the substrate temperature. Immediately after each run the films were heat-treated for several hours at about 100 °C in vacuum in an attempt to anneal out any non-equilibrium structural stresses.

High density polyethylene (HDPE) films of thickness of about 25 μm, free of antioxidants and other additives were used for this investigation. The film was first cut into pieces of the size 2.5 cm square, and one piece was then placed on each of the substrates which had already been mounted on the bottom electrode surface. Nitrogen and SiH4 were used as foreign elements. The plasma implantation parameters for polyethylene films incorporated with nitrogen and silicon are given in Table 5.1. The plasma for both cases was very stable. The substrate temperature was about 20 °C below the melting point of the films which was 145 °C.

We use infrared spectrometry to check the impurity content in the impurity incorporated films. The infrared

spectrum for polyethylene films incorporated with nitrogen by plasma implantation is shown in Figure 5.2. The incorporation of nitrogen in polyethylene gives rise to two new absorption bands in the vicinities of 1600 cm and 2200 cm, which correspond to the stretching bands of the C-N bond and the C-N bond, respectively [46]. The infrared spectrum for pure polyethylene films is also shown in Fig. 5.2 for comparison purposes, and is similar to that reported by other investigators [46].

The infrared spectrum for polyethylene films incorporated with silicon by plasma implantation in a gas mixture of 10% SiH and 90% H (volume concentration) is shown in Fig. 5.3. The incorporation of silicon in polyethylene gives rise to three new absorption bands in the vicinities of 780 cm , 840 cm , and 1020 cm which correspond to stretching bands of the SiC, SiH, and SiH bonds, respectively [47]. Figures 5.2-5.4 show clearly that elements can be incorporated into a polymer by plasma implantation.

We have also produced polyethylene films incorporated with hydrogen by the same plasma implantation technique in a pure hydrogen gas which was used as the pure specimen in this experiment. The incorporation of hydrogen in polyethylene does not affect the infrared spectrum of the polyethylene.

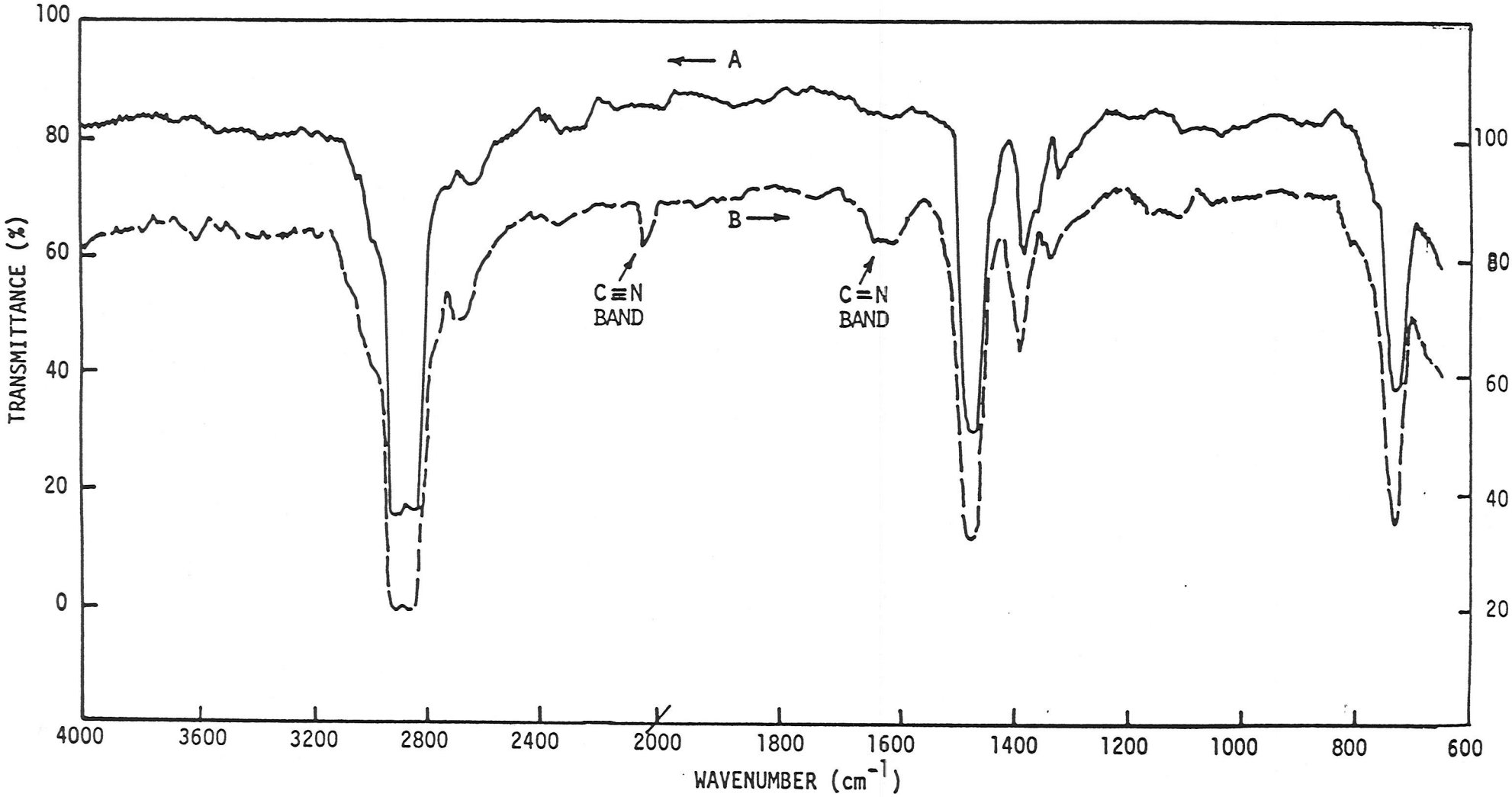

Fig. 5.2: Infrared spectra of (A) pure polyethylene film, and (B) polyethylene film incorporated with nitrogen.

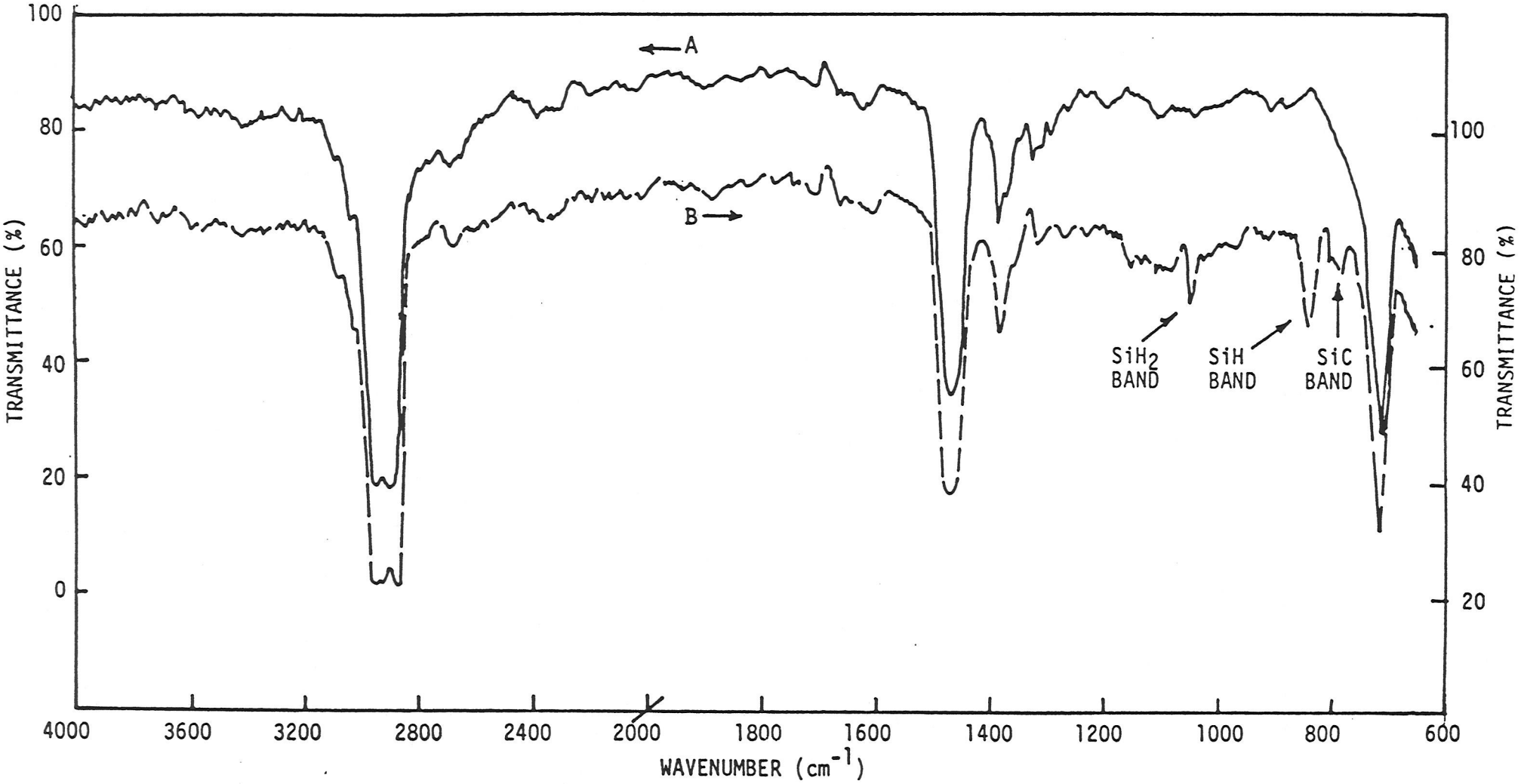

Fig. 5.3: Infrared spectra of (A) pure polyethylene film,and (B) polyethylene film incorporated with silicon.

Since the specimens have thickness of 25 μm which is too thick for the self-healing technique to be used for breakdown strength measurements, we used the simple experimental arrangement as shown in Fig. 5.4A for these measurements.

The rise time of the applied dc voltage is very important since it is related to the time required for a certain density of space charges to build up. For this investigation we used 10 kV/18s, which was the highest speed we could use because of the limit of the voltage rise speed controller.

For each temperature or concentration more than 50 specimens were used for breakdown strength measurements. The thickness of each sample was measured by Surface Profile Measuring System (Sloan Dektak). After measuring the breakdown voltage and sample thickness, the breakdown strength was calculated. The distribution of breakdown strengths follows a Gaussion type distribution as shown in Fig. 5.4. Thus the data to be presented in the next section are the average breakdown strengths with standard deviation.

5.2 EXPERIMENTAL RESULTS

Figure 5.5 shows the breakdown strength of nitrogen incorporated films as a function of nitrogen concentration. The breakdown strength increase with increasing nitrogen concentration.

Figure 5.6 shows the breakdown strength of nitrogen incorporated and pure polyethylene films as functions of temperature. The films incorporated with nitrogen give a higher breakdown strength than the pure polyethylene film, and this difference increases as the temperature is increased. Figure 5.7 shows the percentage of such a difference (ΔE) as a function of temperature, being defined as:

$$\Delta E=(E_b-Ep)/Ep$$

where Eb is the breakdown strength of the polyethylene film incorporated with impurities and Ep is the breakdown strength of the pure polyethylene film.

For the silicon incorporated polyethylene films the breakdown strength becomes lower than that of the pure polyethylene films at room temperature. In Table 5.1 lists the breakdown strengths of pure, nitrogen incorporated and silicon incorporated polyethylene films at room temperature.

5.3 DISCUSSION

Polymers are generally low mobility insulating materials. No conventional breakdown theory is adequate to explain all breakdown phenomena in polymers. However, the new theory proposed by Kao [21] can explain our experimental results. Kao's theory states that breakdown in low mobility insulating materials involves the creation of low-density

Table 1. Plasma implantation parameters.

Parameter	Polyethylene films incorporated with nitrogen	Polyethylene films incorporated with silicon
Gas Mixture	N_2 and H_2	SiH_4 and H_2
Radio-frequency power (w)	30	20
Substrate temperature (°C)	120 ~ 125	125 ~ 135
Bottom electrode dc bais (V)	-90	-70
Chamber pressure (Torr)	1-2	0.1

Table 2. Some Breakdown Strength of polyethylene (PE) films incorporated with nitrogen and silicon.

Film Sample (temperature 20 °C)	Breakdown Strength (MV/cm)
Pure PE	4.97
PE incorporated with nitrogen	5.68
PE incorporated with silicon	3.63

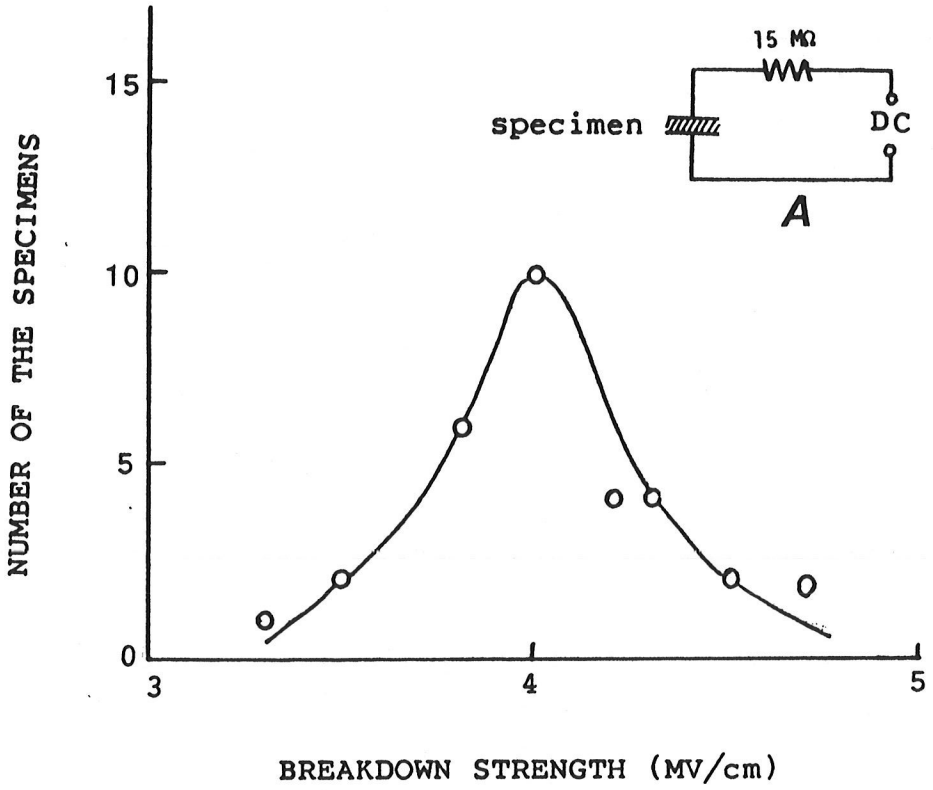

Fig. 5.4: The distribution of breakdown strength.

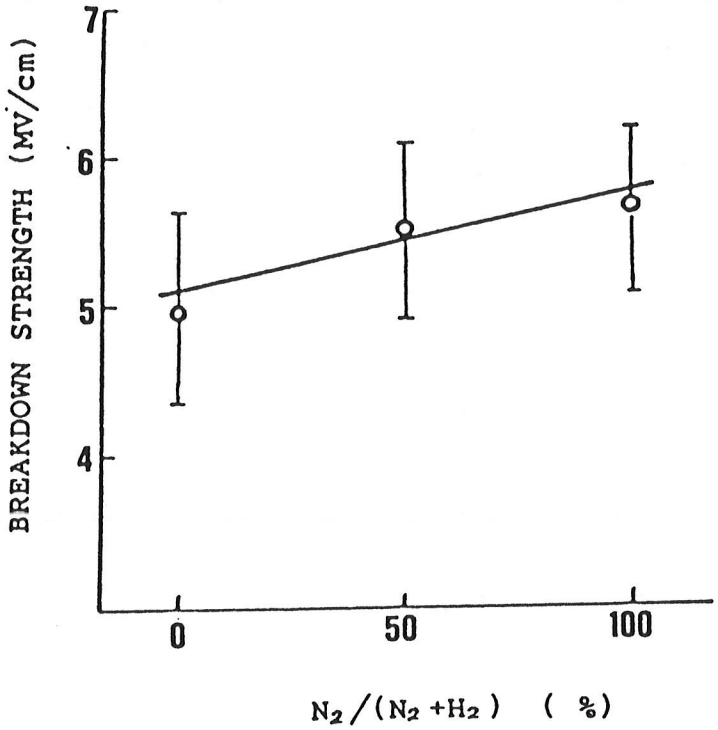

Fig. 5.5: Variation of breakdown strength with nitrogen concentration. (the volume ratio of $N_2/(N_2+H_2)$ in the gas mixture for plasma implantation).

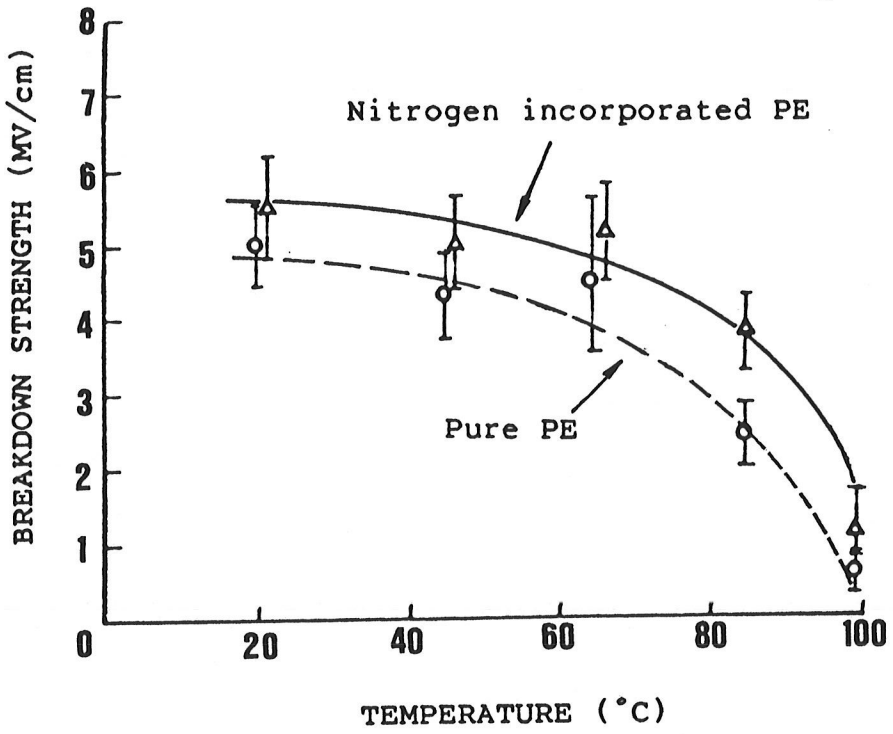

Fig. 5.6: Breakdown strength of nitrogen incorporated polyethylene film and pure polyethylene film as functions of temperature.

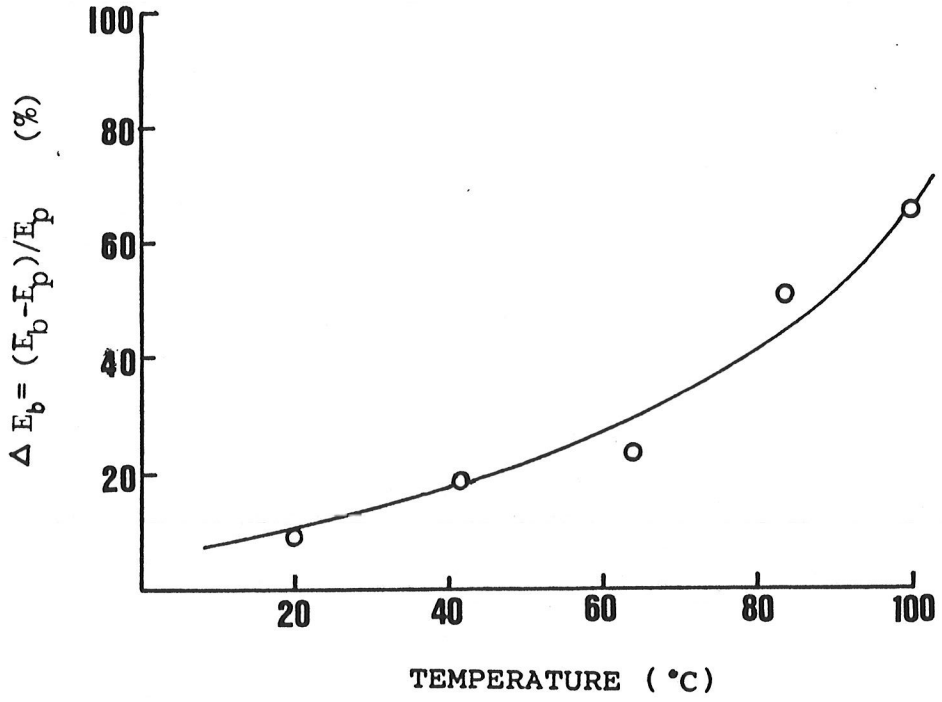

Fig. 5.7: The difference between E_b (breakdown strength of nitrogen incorporated polyethylene films) and Ep (breakdown strength of pure polyethylene films) as a function of temperature.

domains or channels in the bulk by carrier injection from electrical contacts and subsequent dissociative trapping and recombination.

The impurities incorporated into a polymer would introduce new localized states in the polymer. That nitrogen incorporated polyethylene gives a higher breakdown strength may be explained as being due to the introduction of shallow traps which tend to reduce the energy of hot electrons. In this case the bond breaking may involve a multiple hot-electron bombardment process which reduces the probability for the generation of high energy hot electrons, thus leading to an increase in the threshold voltage for the onset of discharge or breakdown in polyethylene. The breakdown strength of the nitrogen-incorporated film increases with increasing nitrogen concentration at room temperature as shown in Fig. 5.5. This implies that the more shallow traps that exist, the lower is the probability for the injected electrons to break the bond.

As temperature increases, recombination is more likely to be non-radiative, thus the total energy released from the trapping and recombination process will increase. Furthermore, the higher the temperature, the less the energy is required to break the bonds. This explains why the breakdown strength difference between nitrogen-incorporated and pure polyethylene films (ΔE) increases as the temperature is increased.

Polyethylene is a linear polymer, and impurities incorporated into polyethylene will produce more crosslinking. Crosslinking will play two roles in polyethylene; one is to make the chemical bond more difficult to break, and the other is to increase Young's modulus of elasticity in the high temperature region, so that the impurity incorporated film will be less compressable than the undoped film [48]. It is likely that crosslinking tends also to increase the breakdown strength.

It can be imagined that such an increase in breakdown strength will finally reach a saturation valve at an optimal concentration of impurities. It is important to find such an optimal concentration for different types of impurities.

Polyethylene incorporated with silicon is quite different. In this case silicon may introduce deep rather than shallow traps in polyethylene films. According to Kao's model, deep traps will not help to increase the breakdown strength. In fact the breakdown strength of the polyethylene incorporated with silicon is lower than the pure polyethylene films at room temperature. To explore further the role played by silicon in polyethylene, more experimental results revealing the effects of incorporated silicon on both the electrical and optical properties are necessary.

5.4 CONCLUSIONS

(1) Polyethylene incorporated with nitrogen has a higher breakdown strength than the pure film; the polyethylene incorporated with silicon has a lower breakdown strength than the pure film.

(2) The increase in breakdown strength due to the incorporation of nitrogen in polyethylene's rubber-like state is attributed to shallow traps created by the impurities.

(3) These experimental results are indirectly in support of the theory put forward by Kao. To prove this model directly, further research is required to study how hot electron transfer can be produced through the energy transfer process.

Chapter VI

ELECTRIC CONDUCTION IN POLYETHYLENE BETWEEN CONDUCTIVE FLUID ELECTRODES

It is well known that because of the morphology of polymer structures, most fluids of low viscosity are penetrable into polymers [49,50,51]. Some fluids such as acetophenone and dodecanol used as additives have the capability of inhibiting tree initiation or growth in polyethylene. Additives having such a capability are attractive to the insulation industry because the inhibition of tree initiation or growth implies the extension of the service life of polymeric-insulated apparatus and systems. It is generally believed that trees are initiated in regions of highly localized electric fields, and that the action of additives is a stress grading process activated either by field-enhanced dissociation [8,9] or by field-enhanced ionization [10]. Although such a stress-grading mechanism has long been used to elucidate the tree inhibition phenomenon, it is not unique and also not consistent with other features related to this phenomenon. To examine the stress-grading mechanism and to probe other more appropriate mechanisms, we have carried out an investigation into this problem from a

different angle by studying electric conduction in polyethylene between conductive fluid electrodes, since understanding the mechanisms of conductivity in polymers would provide further insight into the behaviour of additives in polymers.

6.1 EXPERIMENTAL DETAILS

The test cell holding the conductive fluid used as electrodes is shown schematically in Fig. 6.1. The cell was made of teflon and consisted of two identical parts. The polyethylene film sample was clamped between the two parts forming fluid containers on both sides of the sample, which were well sealed against leaks. A stainless steel mesh with a window size of about 0.5 mm square was used to make a metallic contact with the polyethylene sample surface on each side. This mesh contacts was also used to measure the potential across the sample. On both sides a copper plane of 2 cm in diameter, located at a distance of 5 mm from the sample surface and locked in position by means of teflon spacers was used as the electrode. The diameter of the fluid-polyethylene surface contact area was 2 cm. The fluid was injected into the test cell through glass tubes as shown in Fig. 6.1. The thickness of the polyethylene film was 25 μm.

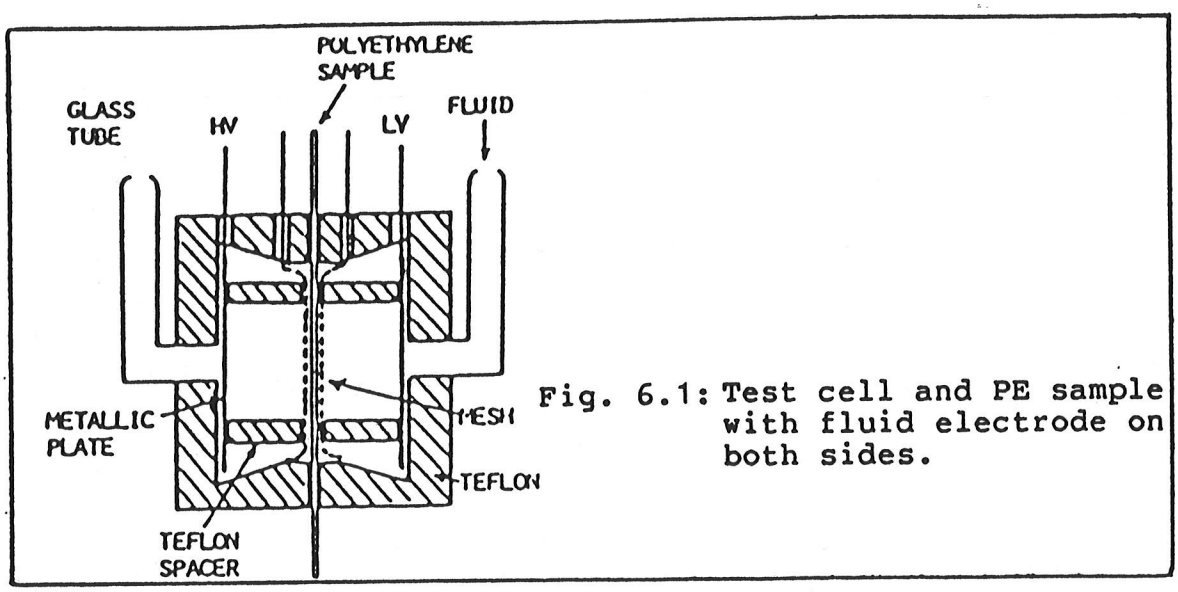

Fig. 6.1: Test cell and PE sample with fluid electrode on both sides.

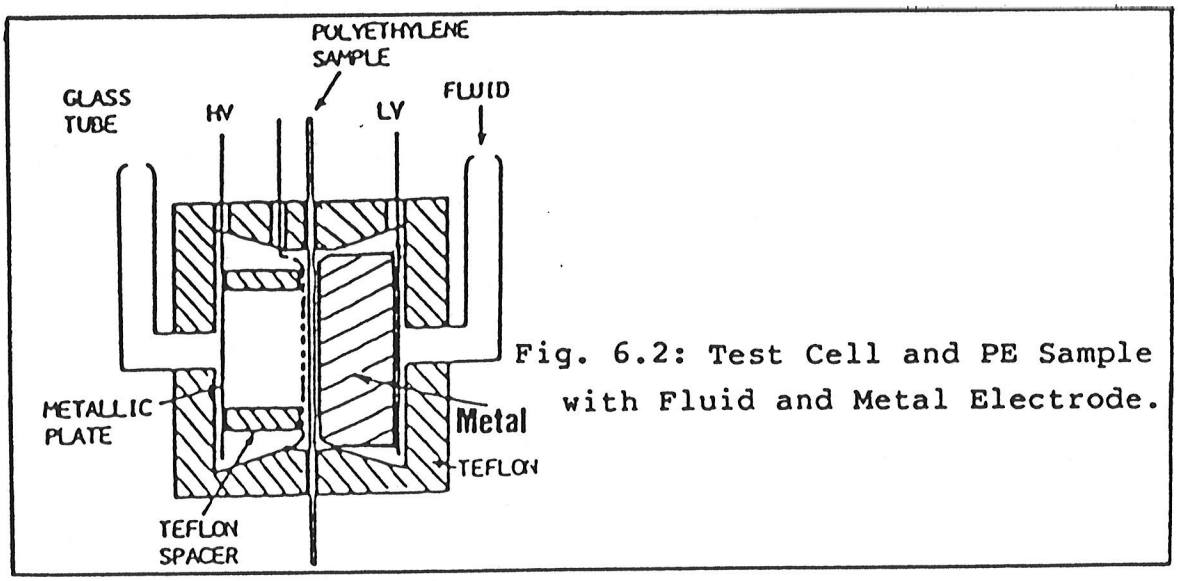

Fig. 6.2: Test Cell and PE Sample with Fluid and Metal Electrode.

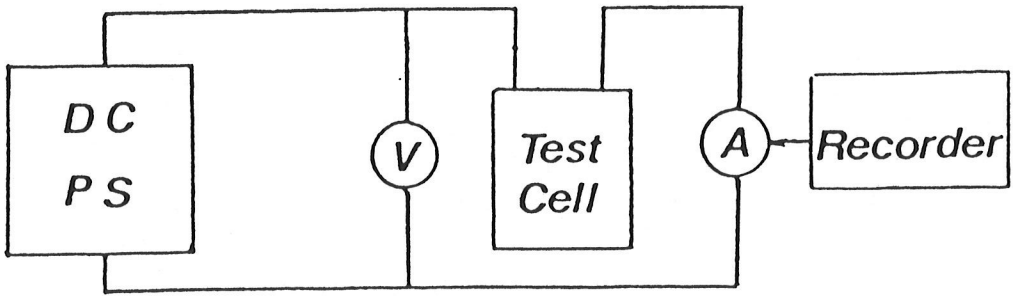

Fig. 6.3: Experimental Circuit Arrangement.

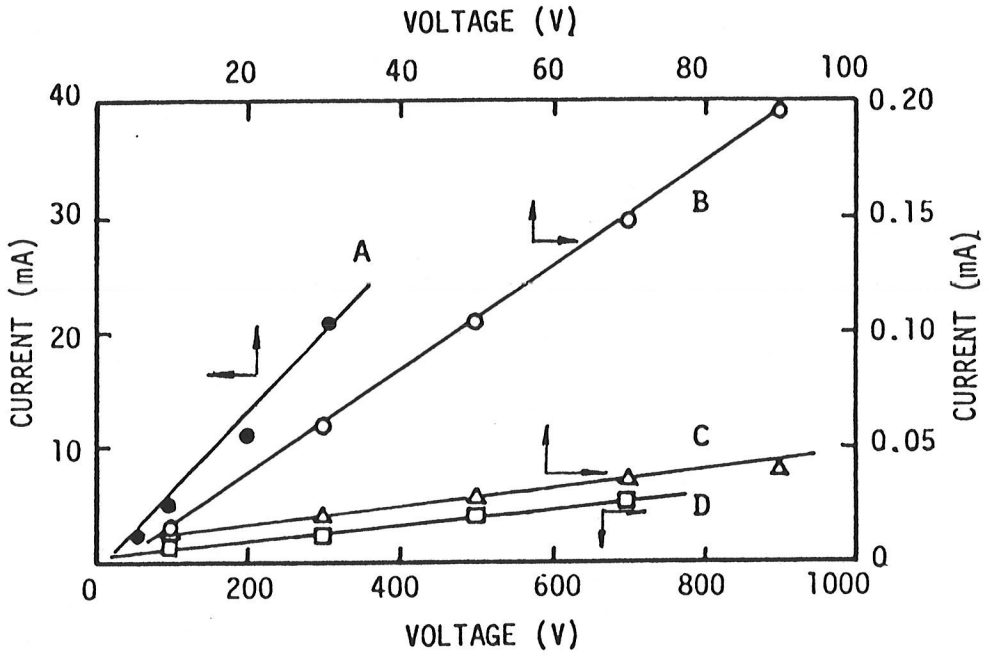

Fig. 6.4: The current-voltage characteristics of liquids. A, water; B, butanol; C, acetophenone; D, dodecanol.

To study polarity effects, we used a fluid electrode on one side and a vacuum-deposited aluminum electrode on the other side as shown in Fig. 6.2.

The conduction current was measured as a function of the field. The constant voltage source was a DC supply providing voltages from 100 V to 5000 V. The measuring system consisted of a potential meter and a current recorder, by which the conduction current could be recorded automatically. The experimental circuit arrangement is shown in Fig. 6.3.

The injected current density after the application of a constant voltage varied with time. The steady state current was measured after the sample had been electrically stressed for one hour to ensure that the current was practically invariable with time. Prior to the increase of the voltage to a higher value, the sample was short-circuited for about one hour in order to get rid of any stored charges in the fluid and sample.

Before any measurements, care was taken to ensure the area of polyethylene sample under investigation was free of mechanical pinholes. The sample was examined under a microscope of 200x magnification to check noticeable defects; and tested between two metallic electrodes at an applied voltage of 100 V, if the current was less than 10 nA the sample was considered to be free of pinholes [52].

Four fluids were used for electrodes, and they are acetophenone, butanol, dodecanol and water. Acetophenone and dodecanol have been used as good additives to add to polyethylene to inhibit electrical tree initiation. Butanol has the same structure as the dodecanol and water is a good ion source. These fluids were not specially treated but before being used their conductivities were measured using two parallel-plane stainless steel electrodes shaped to give Bruce-type uniform field electrodes with an over-all effective diameter of 1 cm. The conductivities are 7.4×10^{-9}, 2.6×10^{-8}, 4.9×10^{-10} and 2.7×10^{-4} $s\cdot cm^{-1}$ for acetophenone, butanol, dodecanol and water, respectively. At low voltages the conductivity of the liquid does not change with the voltage, as shown in Fig. 6.4. We also use these liquids as one electrode and metal as the other electrode to test the polarity effect on the conduction current. The last step of the experiment was to purify acetophenone and to use it as the liquid electrode to compare with the case without purifying treatment.

6.2 EXPERIMENTAL RESULTS

The time dependence of the conduction current in polyethylene film is shown in Fig. 6.5. The conduction current voltage (I-V) characteristics of polyethylene films for four different fluid electrodes are shown in Fig. 6.6. It is interesting to note that the conduction current is dependent

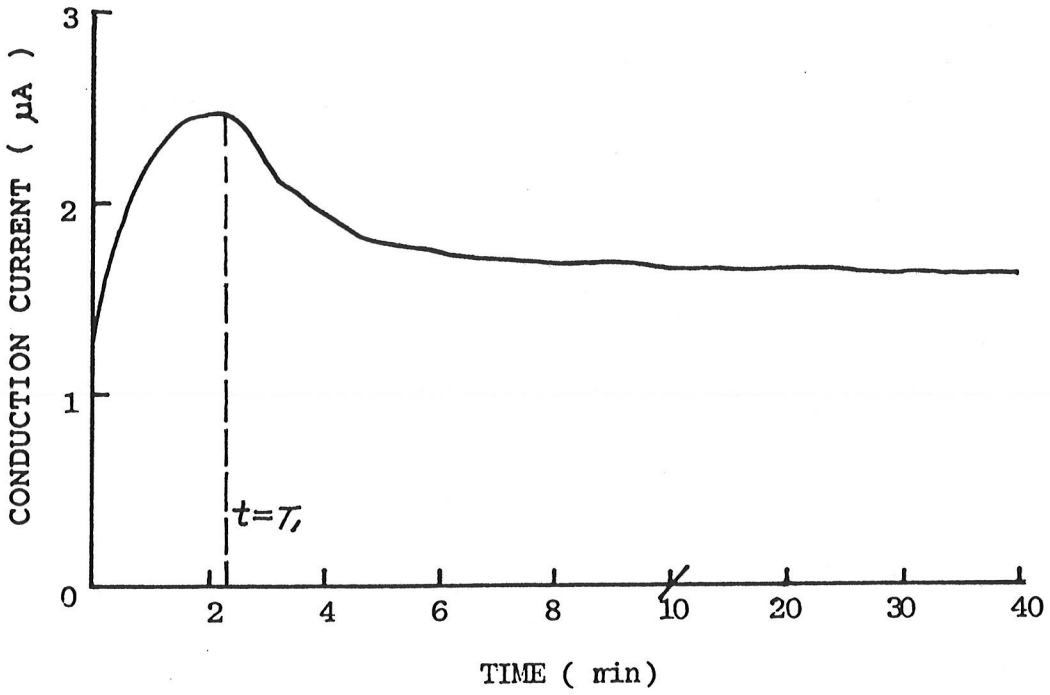

Fig. 6.5: The typical time dependence of conduction current in the polyethylene film.

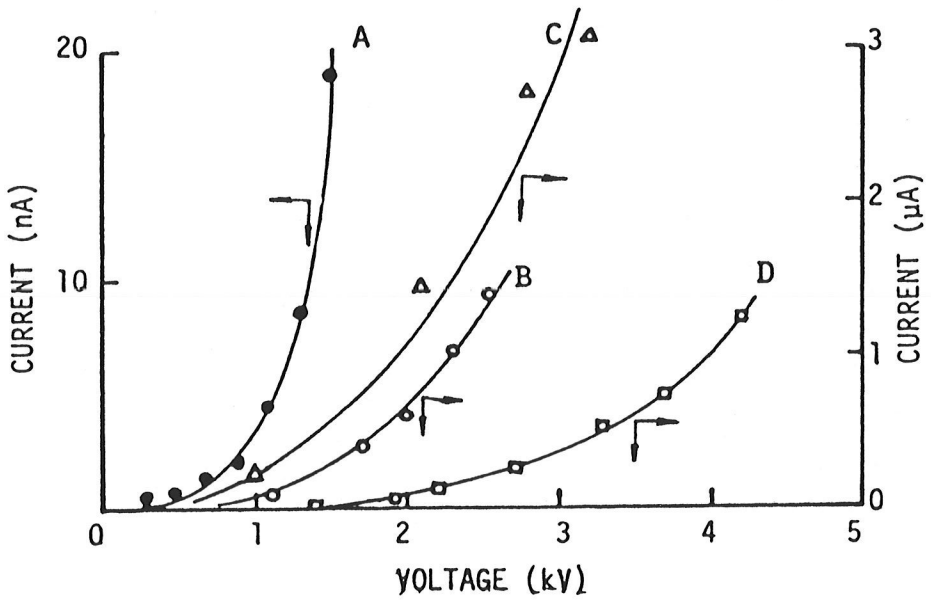

Fig. 6.6: The current-voltage characteristics of polyethylene films with both electrodes of (A) water, (B) butanol, (C) acetophenone, and (D) dodecanol.

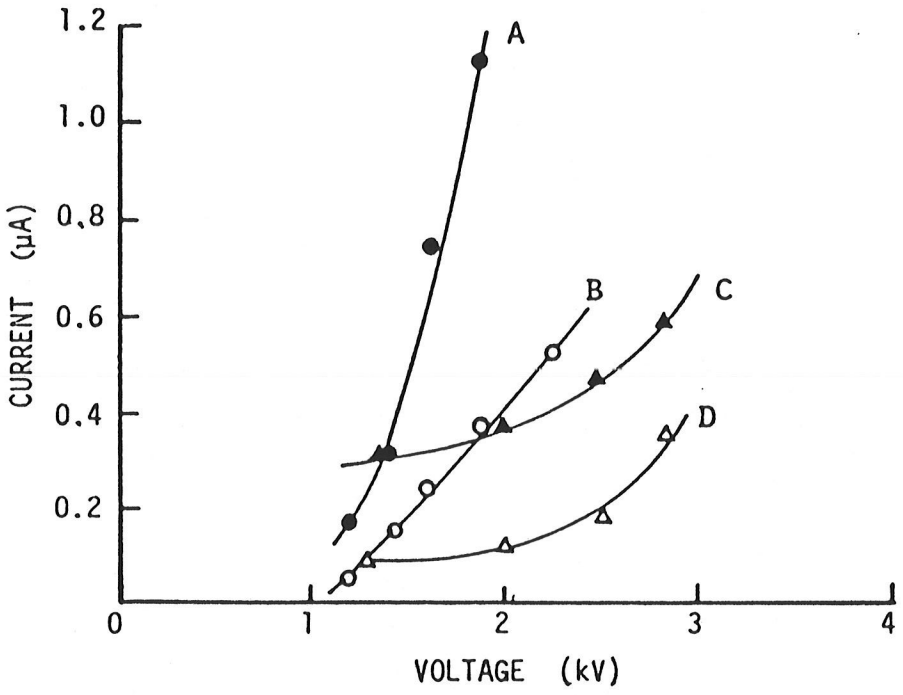

Fig. 6.7: The current-voltage characteristics of polyethylene films with one aluminum electrode and one electrode of (A) - butanol, (B) + butanol (C) - acetophenone, and (D) + acetophenone. The sign - or + represents the polarity of the fluid electrode.

on the liquid. When one of the electrodes is metallic the I-V characteristics of the polyethylene film depends on the polarity of the fluids, especially for acetophenone and butanol; these results are shown in Fig. 6.7. The I-V characteristic of polyethylene films using fluid electrodes are not affected by the metallic mesh in contact with the polyethylene surface. The potential difference across the polyethylene film is practically equal to the applied voltage between electrodes. This implies that the field in the fluid electrodes is negligiblly small.

6.3 DISCUSSION

Fluid electrodes increase the conductivity of a polyethylene film, implying that charge carriers can penetrate into the polyethylene film. However, we still do not know what these carriers are; electrons or ions.

From the experiments, we have observed the time dependence of the penetration current. The penetration current density can be divided into three sections with respect to time. In the first section the initial current is established. In the second section, the initial density increases as a result of the movement of charge carriers through the sample until t=T1, at which the forward edge of the carrier front reaches the opposite electrode. In the third section, the current density decreases as a result of

the formation of a space charge. If the voltage is applied for a long period, then the reservoir of charge carriers in the region of the liquid electrode begins to become exhausted. The time T1 can be considered as the time required for the charge carrier to penetrate through the polyethylene film, so the charge carrier mobility can be calculated from the following equation:

$$\mu = 0.787 \cdot \frac{L^2}{T_1 \cdot V}$$

where L is the thickness of the polymer film, t is the time and V is the applied voltage across the film [53].

The mobility of the charge carriers is about 5×10^{-11}~2×10^{-12} $cm^2/V.s$ when acetophenone, dodecanol and butanol are used as one side electrode. These mobilities are eight to ten orders of magnitude lower than the mobility of electrons in polymers, which is 10^{-3}~10^{-4} $cm^2/V.s$ [53,54].

Figure 6.7. shows that the penetration current depends also on the polarity. For acetophenone and butanol, the penetration current is higher when the fluid is positive than when it is negative. This phenomenon was also observed in water and dodecanol, but the difference is less.

The very low mobility of the charge carriers and the polarity dependence of the penetration current indicates that the conduction current observed is due to ion movement between the polymer free volume and molecular chains.

Another evidence of ionic conduction is that the penetration current is strongly related to the fluid used. The reason for this can be summarized as follows: the work of transport of the ion (W) from the liquid ion source into the polymer is dependent on the difference between the energy of coulombic interaction of the ion in the polymer and that in the electrolyte solution. The larger the size of the ions, the larger is their inertia and hence the higher is the activation energy required for their migration or orientation. This may explain why the current passing through the polyethylene film is higher for acetophenone than for butanol and than for dodecanol (see Fig. 6.6). Water is quite different; it gives the lowest current because the OH ions have a higher inertia due to their highly polar nature.

From all of these experimental results mentioned above, we can conclude that the penetration current is an ionic conduction current. The liquid ions and impurity ions can enter the polymer and move in the free volume.

6.3.1 Models for the Ionic Conduction

All the four fluids are aqueous solutions. There are some oxonium ROH and hydroxide OH ions derived from the solution itself and also a large quantity of various impurity ions in the solution. It is these impurity ions which are respon-

sible for the high liquid conductivities of these solutions. Of course, if the size of the impurity ion is large, it will not be able to penetrate into the polyethylene film and hence can not contribute to the conduction current passing through the film.

In order to examine the effects of impurity ions on the penetration conduction current, we purified the acetophenone by distillation. After three cycles of distillation the conductivity of the acetophenone decreased to 2.8×10^{-10} s·cm^{-1} from 7.4×10^{-9} s·cm^{-1}. Figure 6.8 shows that the penetration current with acetophenone distilled is less than that undistilled, but the conduction current is still very high.

These results imply that the acetophenone molecules may be dissociated into positive and negative ions under high fields, but from the chemical structure the acetophenone molecules are not likely to be dissociated into ions. However, prototropic conduction is possible in these liquids. Prototropic conduction means that the hydrogen ion jumps between the liquid molecules [55], as shown schematically in Fig. 6.9. For acetophenone, the polarized carbon group have $-\delta$ and $+\delta$, thus prototropic conduction may occur. When the liquid molecules enter the polyethylene film, this conduction mechanism will also occur. Since prototropic conduction involves the movement of the hydrogen ions, this conduction is still ionic.

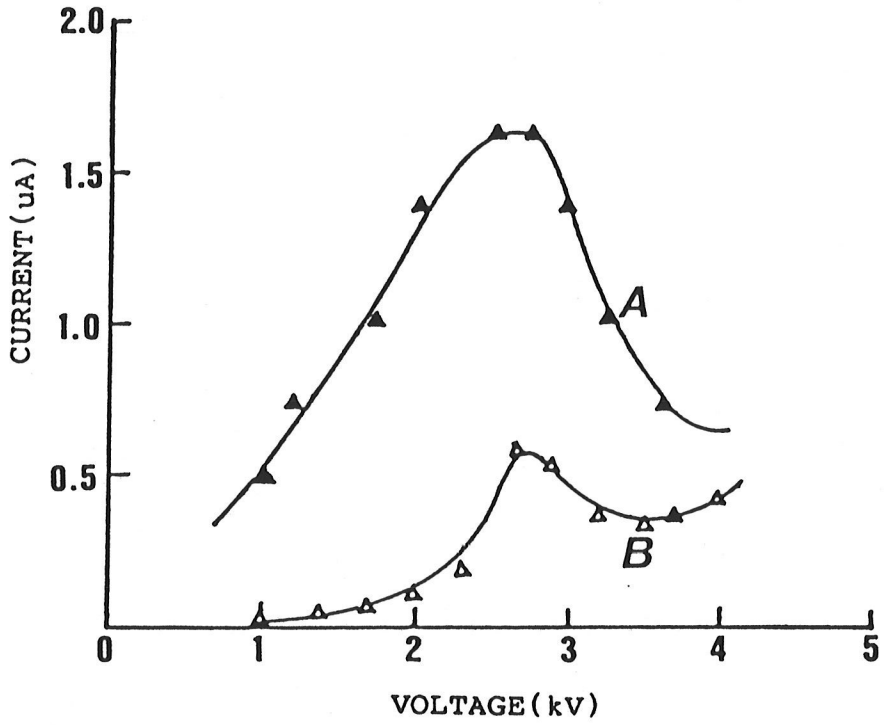

Fig. 6.8: The current-voltage characteristics of polyethylene films with both acetophenone electrodes.
(A) Acetophenone (without distillation)
(B) Acetophenone (with distillation).

Fig. 6.9:

Schematic Process of Prototropic Conduction

WATER

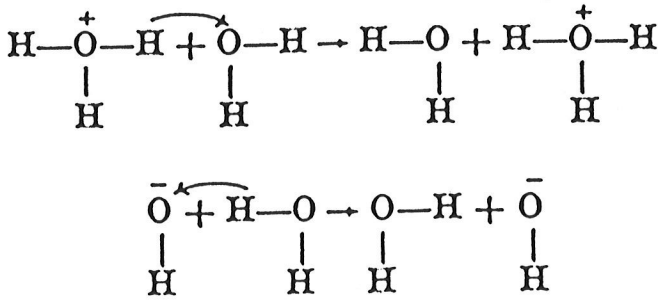

METHANOL

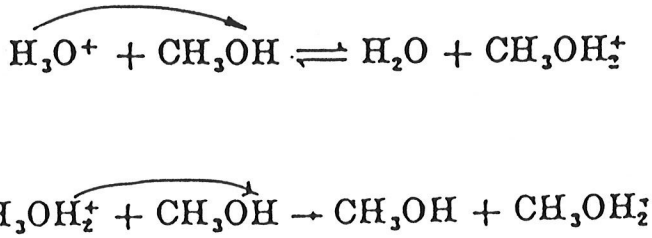

ACETOPHENONE

The polarization of the carbonyl group.

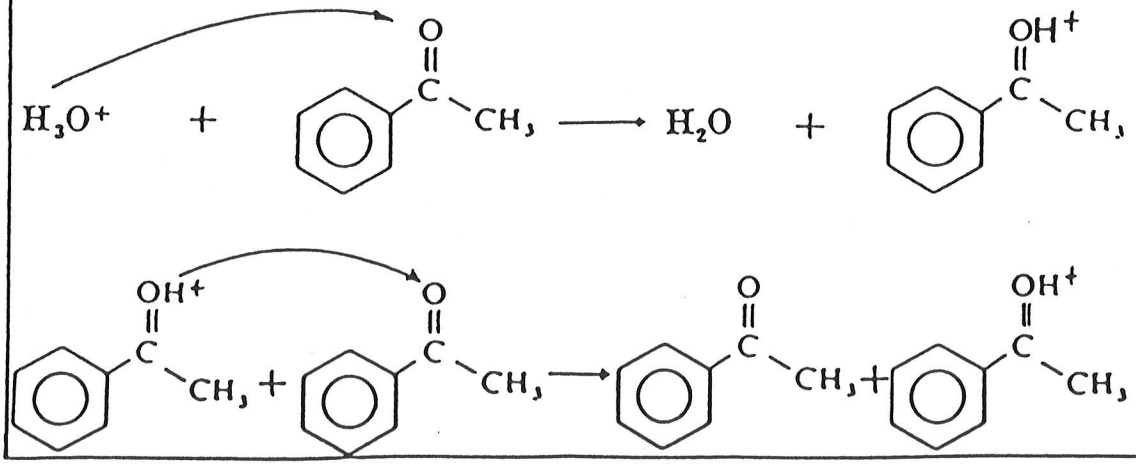

It is therefore likely that the fluid molecules first diffuse into the fibrils of the polyethylene film, i.e. into the free volumes between the individual polymer chains. Then these molecules are dissociated into ROH and OH ions under high fields inside the polyethylene film as shown in Fig. 6.10A. These ions either migrate following the electric field as shown in Fig. 6.10B, or do not involve direct movement, but have their protons transferred from molecule to molecule following the prototropic process as shown in fig. 6.10C.

No matter which process is predominant, the charge movement requires an activation energy because of the energy barrier existing between two equilibrium positions. This is true even for the protonic transfer since the ROH ions have to orient themselves to a favourable angle for such a transfer to occur.

Applied electric fields tend to reduce the barrier height and hence reduce the effective activation energy required for the charge carriers entrance and movement in the polymer. Furthermore, the dissociation energy is much smaller than the ionization energy for these four fluids. We believe that the charge carriers are mainly ions which are produced by the dissociation of the fluids molecules under high field. Therefore, the current is expected to increase more rapidly at higher fields as shown in Fig. 6.3.

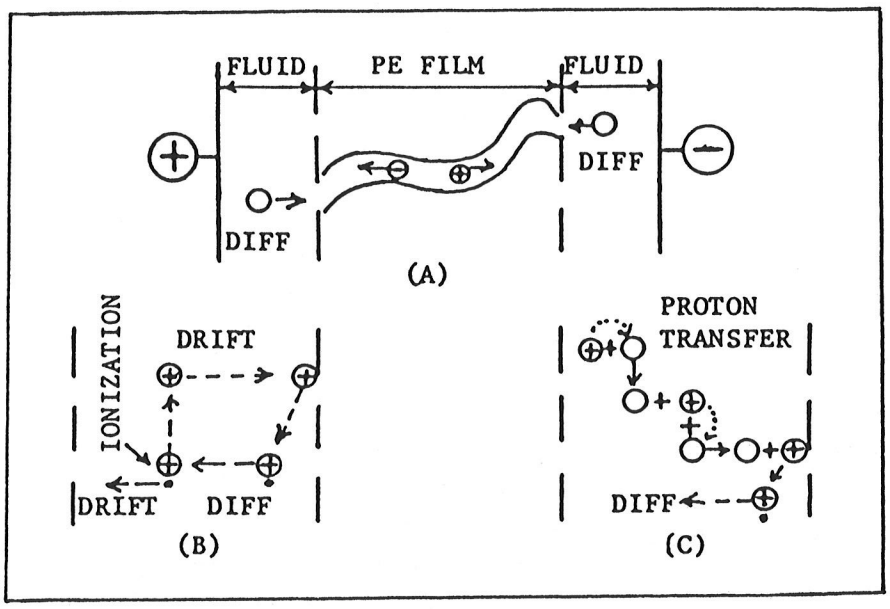

Fig. 6.10: (A) Molecule diffusion into PE film, (B) ion migration, and (C) prototropic process $ROH_2^+ \cdots\cdots\rightarrow ROH \longrightarrow ROH + ROH_2^+$.

It is interesting to note that the penetration current of acetophenone in polyethylene has a peak around 2800 V. This peak may be due to the space charge accumulated in the polymer chains, since electric hysteresis was found around 2800 V.

6.3.2 A New Mechanisms for Additives

On the basis of the above results we do not believe that the additives of acetophenone or similar materials in polymers would provide a stress-grading effect. Taking a point-plane electrode configuration as an example, there are two ways to relieve the high stress near the point tip: (1) the formation of a homo space charge or, (2) the formation of a high-density plasma (a mixture of positive and negative charge carriers with zero total charge) around the point tip. These two processes can not occur under dc fields if the charge carriers are generated in the bulk. In fact, the addition of acetophenone in polyethylene tends to increase both the dc tree initiation voltage and the dc breakdown voltage when the point is positive, but to decrease them when it is at negative polarity [32]. This phenomenon does not support the stress grading mechanism.

The effects of additives in polymers can be well explained on the basis of Kao's theory [21]. The additive under dc fields produces a hetero-space charge close to the

point electrode, thus enchancing the carrier injection. This action tends to deteriorate the treeing properties. However, the additives also create shallow traps which tend to reduce the energy released due to trapping and recombination, thus reducing the probability of forming low-density regions. This action tends to improve the treeing properties. If the former action is predominant, the additive will decrease the tree initiation voltage, but if the latter action is predominant, it will increase the tree initiation voltage.

6.4 CONCLUSIONS

(1) Acetophenone and its impurities can penetrate into, and migrate through polyethylene.

(2) Electric conduction in polyethylene with acetophenone as an additive is due to the movement of impurity ions and prototropic transport in acetophenone.

(3) There is no indication of electron impact ionization in high field conduction in polyethylene added with acetophenone.

(4) The role played by the acetophenone in polyethylene is to create more shallow traps rather than to produce electric field stress-grading.

Chapter VII

CONCLUSIONS

On the basis of the experimental studies described above, the following conclusions are drawn:

(1) The oxide layer at the interface between a polymer and metallic contact suppresses the direct communication between the carrier injecting contact and the polymer, and reduces the efficiency of carrier injection into the polymer.

(2) In polyethylene, hole injection is as feasible as electron injection from the point electrode.

(3) Computer simulation of polarity effects on the discharge patterns indicate that the discharge patterns are not always governed by a deterministic field-dependent process but also in some cases by a stochastic process.

(4) Foreign elements incorporated in polyethylene affect the breakdown properties. This effect can be interpreted as being due to new localized states created by the foreign elements, which modify the amount of energy released in trapping or recombination processes.

(5) Additives in polyethylene is to influence the trap distribution rather then to produce electrical field stressing grading. The additives become dissociated under high fields, thus resulting in ionic or prototropic conduction in polyethylene.

The immediate research program to follow after this thesis is to study experimentally and theoretically the actual roles played by incorporated impurities in polymers. To study these, we plan to systematically measure the dark conductivity and photo conductivity, thermal stimulated current, photoluminescence, refractive index and absorption over a wide range of wavelengths. We also plan to study their structures by means of X-ray diffraction and electron microprobe analysis. We shall concentrate on the study of three polymers; namely polyethylene, P.V.K. and polyacetylene, with and without the incorporation of foreign elements. To start with, nitrogen and silicon will be used. We also plan to study the physics behind the empirical parameters used in the computer simulation of discharge patterns.

REFERENCES

1. E.J. McMahon, "A tutorial on treeing", IEEE Trans. Elec. Insu. Vol. EI-13 No 4, pp 277-288, 1978.

2. M.T. Shaw and S.H. Shaw, "Water treeing in solid dielectrics", IEEE Trans. on Elec. Insu. Vol. EI-19 No.5, October 1984.

3. R.M. Eichhorn, "Treeing in Solid Extruded Electrical Insulation", IEEE Trans Elec. Insu.,Vol. EI-12, No. 1, p.2-18, (1976).

4. B.Mandelbrot, "The Fractal Geometry of Nature", W.H. Freeman, San Francico, 1982.

5. L. Pietronero and H.J. Wiesmann, J. Stat. Phys. 36,909 , 1984.

6. M. Ozaki, D. Peebles, B.R. Weinberger, A.J. Heeger and A.G. MacDiamid, "Junction formation with pure and doped polyacetylene", Appl. Phys. Lett., Vol.35, 1979, pp.83-85.

7. E.J. McMahon, "A tree growth inhibiting insulation for power cable", IEEE Trans on Elec. Insu. Vol. EI-16 No.4, pp.304-318, 1981.

8. J.C. Devins and S.J. Rzad, 1975 Annual Report-CEIDP, National Academy of Science (Washington,D.C.), pp. 344-353, 1975.

9. D.M. Tu, L.H. Wu, X.Z. Wu, C.K. Cheng and K.C. Kao, IEEE Trans. Elec. Insu. Vol. EI-17, pp. 539-545, 1982.

10. S.J. Rzad and J.C. Devins, 1978 Annual Report-CEIDP, National Academy of Science (Washington,D.C.), pp. 352-360,1982.

11. K.C. Kao and W. Hwang, "Electrical Transport in Solids", Pergamon Press, Oxford, 1981.

12. D.A. Seanor, "Electrical Properties of Polymers", Academic Press, New York, 1982.

13. M. Ieda, "Electrical conduction and carrier traps in polymeric materials", IEEE Trans on Elec Insu Vol. EI-19 No.3, pp.162-178, June 1984.

14. K.W. Wargner, "The physical nature of the electrical breakdown of solid dielectrics", AIEE Trans. Vol. 41, 1922, pp. 288-299.

15. W. Rogowski, "Der elektrische Durchschlag von gasen, festen und flussigen isolatoren", Arch. Elektrotech. Vol. 19, 1930, pp. 569-578.

16. A. von Hippel, "Electric Breakdown of Solid and Liquid Insulators", J. Appl. Phys. Vol. 8, 1937. pp. 815-832.

17. C. Zener, Proc. Roy. Soc., A.145, 523, (1935)

18. W.Z. Franz, Phys., 113, 607, (1939).

19. F. Seitz, Phys. Rev. 76, 1376 (1949).

20. W.R. Heller, Phys. Rev.84(1951) 1130.

21. K.C. Kao, "New theory of electrical discharge and breakdown in low- mobility condensed insulators", J. Appl. Phys. Vol.55, pp.752-755, 1984.

22. M. Ieda, "Dielectric Breakdown Process of Polymers",IEEE Trans on Elec. Insu. Vol. EI-15 No.3 pp.206-224, 1980.

23. D.W. Kitchin and O.S. Pratt, "An Accelerated Screening Test for Polyethylene High-Voltage Insulation", AIEE Trans Paper 62-54.

24. M. Olyphant, "Corona and Treeing Breakdown of Insulation", The Lake Publishing Company, Volume 9, No.2,3 and 4, 1963.

25. E.J. McMahon and J.R. Perkins, "Surfaces and Volume Phenomena in Dielectric Breakdown of Polyethylene", IEEE Trans Paper 63-181.

26. Vahlstrom, W., Paper presented at IEEE Conference on Underground Distribution, Detroit, Mich., Sept. 1971.

27. J.H. Lawson and W. Vahstrom IEEE Trans PSA 92 824 ,1973.

28. M. Ieda, M. Nawata, 1972 Annual Report, Conf. Elec. Insu. and Dielec. Phen. , Nat. Acad. Sci., Washington,D.C., 1973, p.143.

29. B. Yoda, M. Sakaba, Hitachi Rev. 18 (1969), p.406.

30. S. Fujiki, H. Furusawa, T. Kuhara and H. Matsuba, IEEE Paper 71 Tp 195-PWR (1971).

31. J. Artbauer, Z. Kolloid Z. Und, Polymer 202 (1965),P. 15.

32. K.C. Kao, D.M. Tu, L.H. Wu, X.Z. Wu and C.K. Cheng, "On the Mechanism of Tree Initiation in Polymer", IEEE Conf. Rec. of 1982 IEEE Int. Symp. on Elec. Insu. pp.300-305, 1982.

33. T. Tanaka, A. Greenwood, "Effects of Charge Injection and Extraction on Tree Initiation in Polyethylene", IEEE Trans on PAS, Vol. PAS-97, pp.1749-1757, 1978.

34. K.G. Buerger, "On the Interaction of Time-Dependent Space Charge Condition and Initial Breakdown in LDPE", 1984 Annual Report , Conf.on Elec. Insu. and Dile. Phen. pp.175-180.

35. N. Yoshimura and F. Noto, "Effects of Electrode Materials on Tree Initiation in Polyethylene under Switching Surge Conditions", IEEE Trans On Elec. Insu. Vol. EI-18 No.2, pp.120-124, 1983.

36. J.H. Mason, "Breakdown of Solid Dielectrics in Divergent Fields", Proc. IEE, Vol. 102 Pt. C, pp 254-264. 1955.

37. M. Kosaki, N. Shimizu and K. Horii, "Treeing of Polyethylene at 77K" , IEEE Trans. on Elec. Insul. Vol. EI-12, pp. 40-45, 1977.

38. F. Noto, "Tree Initiation in Polyethylene by Application of DC and Impulse Voltage", IEEE Trans. Elec. Insu. Vol. EI-12, No. 1, pp.26-30.

39. M. Ieda and M. Nawata, "DC Treeing Breakdown Associated with Space Charge Formation in Polyethylene", IEEE Trans. Vol. EI-12, 1977, pp.19-25.

40. R.M. Eichhorn, "Laboratory Studies of Treeing in Solid Dielectrics and Voltage Stabilization of Polyethylene", Conf. Rec. 1976 IEEE Int. Symp. EI. June 14-16 pp.213-218, 1976.

41. R. Patsch, "On Tree-Inhibition in Polyethylene", IEEE Conf. Rec. 1978 Int. Symp. on Elec. Insu. pp. 130-133, 1978.

42. M. Kosaki, N. Shimizu, and K. Horii, "Electroluminescence association with charge injection in polyethylene at cryogenic temperature", 1977 Ann. Rep. Conf. Elec. Insu. and Dile. Phen. pp. 752-755, 1984.

43. K.C. Kao, "High field and photoelectric effects in polymers", Conf Rec. of 1985 Int. Conf. on Prop. and Appl. of Diel. Materials held in Xi'an, China.

44. A. Kapitulnik and G. Deutscher, J. Stat. Phys. 36,815 (1984).

45. L. Niemeyer, L. Pietronero and H.J. Wiesmann, Phys. Rev. Lett.(1984).

46. M.Hudis and T. Wydeven, Polymer Letters Edition 13, 549 (1975).

47. Y. Tawada, K. Tsuge, M. Kondo, H. Okamoto, and Y. Hamakawa, J. Appl. Phys. 53, 5273 (1982).

48. K.H. Stark, C.G. Garton, "Electric Strength of Irradiated Polythene", Nature December 24,1955 vol. 176 pp. 1225-1226.

49. S. Matsuoka, "Hypothesis of voids in semicrystalline polymers", J. Appl. Phys. Vol. 32, No. 11, November, pp.2334-2336, 1961.

50. D.W. Auckland and R. Cooper, "Investigation of water absorption by electrically stressed polythene", Proc. IEE, Vol. 122, No. 8, pp.860-864 August, 1975.

51. S. Kageyama, M. Ono and S. Chabata,"Microvoids in crosslinked polyethylene insulated cable", IEEE Trans on PAS, Vol. PAS-94, No. 4, pp.1258-1263, July/August, 1975.

52. C.T. Meyer and A. Chamel, IEEE Trans. Elec. Insu. Vol. EI-15, pp. 389-393, 1980.

53. K. Kryszewski, A. Szymanski and J. Swiatek, J. Polymer Sci. C16:3915, 1968.

54. G. Lenguel, J. Appl. Phys. 37: 807, 1966.

55. Erdey-Gruz, T, "Transport Phenomena in Aqueous Solutions", John Wiley and Sons, New York, 1974.